The Journal of Chemical Physics

On the thermodynamics of curved interfaces and the nucleation of hard spheres in a finite system

Cite as: J. Chem. Phys. **156**, 014505 (2022); https://doi.org/10.1063/5.0072175
Submitted: 20 September 2021 • Accepted: 15 December 2021 • Published Online: 06 January 2022

P. Montero de Hijes and C. Vega

The Journal of Chemical Physics ARTICLE scitation.org/journal/jcp

On the thermodynamics of curved interfaces and the nucleation of hard spheres in a finite system

Cite as: J. Chem. Phys. 156, 014505 (2022); doi: 10.1063/5.0072175
Submitted: 20 September 2021 • Accepted: 15 December 2021 •
Published Online: 6 January 2022

P. Montero de Hijes and C. Vega[a]

AFFILIATIONS

Departamento de Química Física, Facultad de Ciencias Químicas, Universidad Complutense de Madrid, 28040 Madrid, Spain

[a]Author to whom correspondence should be addressed: cvega@quim.ucm.es

ABSTRACT

We determine, for hard spheres, the Helmholtz free energy of a liquid that contains a solid cluster as a function of the size of the solid cluster by means of the formalism of the thermodynamics of curved interfaces. This is done at the constant total number of particles, volume, and temperature. We show that under certain conditions, one may have several local minima in the free energy profile, one for the homogeneous liquid and others for the spherical, cylindrical, and planar solid clusters surrounded by liquid. The variation of the interfacial free energy with the radius of the solid cluster and the distance between equimolar and tension surfaces are inputs from simulation results of nucleation studies. This is possible because stable solid clusters in the canonical ensemble become critical in the isothermal–isobaric ensemble. At each local minimum, we find no difference in chemical potential between the phases. At local maxima, we also find equal chemical potential, albeit in this case the nucleus is unstable. Moreover, the theory allows us to describe the stable solid clusters found in simulations. Therefore, we can use it for any combination of the total number of particles, volume, and global density as long as a minimum in the Helmholtz free energy occurs. We also study under which conditions the absolute minimum in the free energy corresponds to a homogeneous liquid or to a heterogeneous system having either spherical, cylindrical, or planar geometry. This work shows that the thermodynamics of curved interfaces at equilibrium can be used to describe nucleation.

I. INTRODUCTION

The thermodynamics of an inhomogeneous system having a curved interface is a topic of interest.[1–18] However, even though the thermodynamic description was developed long ago by Kondo[19] and presented in detail in the classical book by Rowlinson and Widom,[20] to the best of our knowledge, it has not been applied to the description of experimental results. Thus, the theory has been treated in most cases as a "formal" result rather than a result from which one can extract useful information about the system. How is it possible for a system with one component (in the absence of an external field) to have an interface between two phases at stable equilibrium? Equilibrium implies that the chemical potential is the same in both phases. Stable equilibrium means that the system remains in its state even after small perturbations from the equilibrium state. This is possible in the canonical ensemble (NVT) which has constant number of particles N, volume V, and temperature T. In this case, the equilibrium is stable[21–23] since the system may find a minimum in the Helmholtz free energy F. However, this is not possible in the grand-canonical ensemble (μVT) where chemical potential μ, V, and T are constant as was discussed by Lee, Telo da Gamma, and Gubbins[23] and Oxtoby and Evans.[24] In this case, the system may reach equilibrium (equal chemical potential in both phases), but the equilibrium will be unstable as the system reaches a maximum in the grand potential Ω rather than a minimum.[23,24] The same is true in the isothermal–isobaric ensemble (NpT) where pressure p, N, and T are constant, as in this case when the equilibrium is reached (i.e., identical chemical potential of both phases), the system reaches a maximum in the Gibbs free energy G and the equilibrium is unstable. Therefore (for one component systems), NpT and μVT are not appropriate ensembles to study the thermodynamics of curved interfaces, simply, because the system never finds stable equilibrium for them. Thermodynamics deals with stable equilibrium, and therefore, the natural ensemble to study curved interfaces is the canonical

one. In fact, the theoretical description of curved interfaces used by Kondo, and Rowlinson and Widom, is developed for a system at constant N, V, and T.

In 1984, Rowlinson-Gubbins and co-workers performed a beautiful study of a droplet of liquid in contact with its vapor for the Lennard-Jones system.[7] In addition, Vrabec and co-workers studied the same system in more detail.[9] In the last 20 years, Binder and co-workers have studied curved interfaces, not only for a curved interface between two fluid phases but also between a solid and a fluid.[2,5,25–33] It is also clear that among all of the curved interfaces, the spherical interface is probably the most important one. Thus, simulations have been useful in obtaining stable curved interfaces for a large number of problems. However, again, one rarely sees the application of the formalism of Kondo[19] when describing curved interfaces in simulations or experiments.

There is another reason to study spherical interfaces. We have recently shown (for a one component system) that when the stable spherical interface (obtained in the NVT ensemble) is studied in the NpT ensemble, then half of the time the system transforms into the external phase and the other half into the internal one.[34–36] When studying nucleation, one usually defines the critical nucleus as that for which the probability of evolving to the phase of the nucleus is one-half and the probability of evolving to the external one is the other half. Thus, the stable spherical solid cluster found in the NVT simulations is a critical nucleus in the language of nucleation. In other words, the same physical system having a spherical interface can be regarded as being at equilibrium or as being critical, simply by changing the ensemble at which it is considered. Thus, the language of the thermodynamics of curved interfaces (which describes the stable equilibrium in the NVT ensemble) can rigorously be used in the context of nucleation (that describes unstable equilibrium in the NpT ensemble). Although this connection seems obvious now and has been confirmed by simulations for several systems as bubbles,[34] drops,[36] or solids clusters,[35] we believe that is it not widely known in the literature although it is likely that this connection has being on the air for some time.[21–24,37–40]

It is interesting to discuss whether a stable interface can be found in other ensembles besides the NVT. To answer this question, it is useful first to imagine a spherical interface at equilibrium (i.e., same chemical potential) as the external phase. Then, imagine that a small perturbation is performed changing the size of the internal spherical phase. If the chemical potential of the external phase is not modified by the perturbation of the internal phase, then the equilibrium will be unstable. This is the case of the μVT and NpT ensembles as in these ensembles changing the properties of the internal phase does not modify the chemical potential of the external phase (which is given by either μ and T or p and T, respectively). However, in the NVT ensemble, if the internal phase is perturbed, the density (and pressure) of the external phase will also be modified, and therefore, the chemical potential will change. For the new chemical potential, the size of the critical cluster will be completely different of that of the perturbed cluster and the system could return to equilibrium (for instance, if the solid cluster increased its size slightly, becoming pre-critical for the new chemical potential, and with the opposite behavior for a fluctuation reducing its size). Another ensemble that allows one to stabilize nuclei (or spherical interfaces) is the isoenthalpic–isobaric (NpH), where enthalpy H, p, and N are fixed but T is allowed to change. In this case, a change in the size of the equilibrium interface (where the chemical potential of both phases is identical) will change the chemical potential of the external phase (since it will change not its pressure but its temperature). In fact, equilibrium solid clusters in the NpH ensemble were obtained by Zepeda-Ruiz *et al.*[41] In the microcanonical ensemble (NVE), one can also stabilize curved interfaces as changing the size of the equilibrium cluster will modify both T and p so that the chemical potential of the external phase μ will change.

The condition of chemical equilibrium between two bulk phases is reached for a given T at a certain value of p that will be denoted as p_{coex}. This pressure will also be the equilibrium pressure between two phases obtained in the NVT ensemble in the presence of a planar interface. However, when having a spherical interface in the NVT ensemble, it is possible to have stable equilibrium between two phases for several values of p at a certain value of T by changing the radius of the interface. The regions of coexistence in the NVT have been extensively described by Binder and co-workers[2,5,25–33] and by MacDowell *et al.* for the Lennard-Jones fluid.[42,43] Another example can be found in the work of Richard and Speck.[13]

Recently, we studied using computer simulations the case of a spherical crystal formed by hard spheres (HS) in equilibrium with the liquid phase forming a stable curved interface in NVT simulations. In Fig. 1, we show a snapshot of the system. We were able to obtain up to ten different solid stable clusters depending on the thermodynamic conditions N and V.[35] In the case of HS, T only determines the velocities of the particles but it does not affect its residual properties (i.e., the difference between those of the real system and those of an ideal gas). Strictly speaking, our simulations were not for a true HS potential but rather a continuous steep repulsive potential[44] which mimics the properties of hard spheres

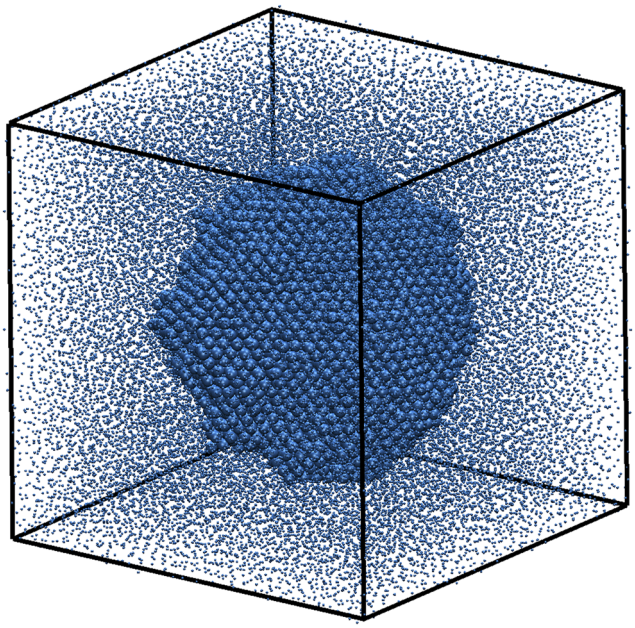

FIG. 1. Snapshot of a stable nucleus in contact with its melt. Solid particles are shown as spheres and liquid ones as points.

TABLE I. Presentation of the ten systems that we shall employ to validate our theoretical approach. The same values of N and V will be applied to the theoretical scheme case by case. The size of the stable nucleus in the simulation is given by $\langle N_{sol}^{sim} \rangle$. These simulations were performed in Ref. 35. We use reduced units for volume (σ^3) and density (σ^{-3}).

Label	V	N	ρ = N/V	$\langle N_{sol}^{sim} \rangle$
I	10 686.4	10 540	0.986 30	1 925
II	20 195.5	19 779	0.979 38	2 736
III	20 195.5	19 829	0.981 85	3 718
IV	49 599.9	48 207	0.971 92	5 604
V	49 599.9	48 357	0.974 94	8 602
VI	108 265.2	104 675	0.966 84	10 498
VII	66 900.1	65 383	0.977 32	15 554
VIII	108 265.2	105 475	0.974 23	23 558
IX	108 265.2	105 875	0.977 92	28 879
X	887 000.0	853 712	0.962 47	129 926

quite well.[44–48] The advantage of using a continuous potential is that one can use standard molecular dynamics programs such as GROMACS[49] or LAMMPS,[50] which are highly optimized. It must be recognized that we obtained our solid clusters by trial and error (combining different values of N and V). This is so because even though we knew that the system, when stable, should be in a minimum in the Helmholtz free energy F, we were unable to determine the value of F for the inhomogeneous system. Therefore, a theoretical framework to understand and predict the size of the stable solid clusters obtained by simulation in our previous work is needed. In an important contribution, Richard and Speck initiated the attempt to obtain via theory an estimate of the size of the spherical solid cluster obtained in NVT simulations for HS.[13] Here, we incorporate some improvements to the theory (and provide some clarifications about the role of pressure as well as its relation with classical nucleation theory). We start validating our scheme by comparing with previous simulation result as well as with a few new results. The parameters of these systems can be found in Table I. We show that this scheme is capable of describing quite accurately the simulation results. Thus, the theoretical treatment helps in understanding the results obtained in our previous simulations and also to extend our description to an arbitrary system in the NVT ensemble. Furthermore, the theory allows us to develop a strategy (better than trial and error as used previously) for searching stable spherical solid clusters in NVT simulations for systems of high practical interest, as it is the case of water. Since we anticipate further research on the area of stable spherical solid clusters in NVT simulations, we believe that the theoretical treatment presented here may be of interest for future studies. In Sec. II, we shall describe briefly the thermodynamics of curved interfaces.

II. THERMODYNAMICS OF CURVED INTERFACES AT EQUILIBRIUM

We shall briefly summarize the thermodynamics of curved interfaces as described by Kondo *et al.*,[19,51] Rowlinson-Widom,[20] and Mullins.[52] We shall focus on the case of the spherical solid clusters. Let us assume that one has a spherical solid cluster in contact with the liquid at equilibrium in a system at constant N, V, and T. Since the system is stable, it must be at a minimum in the Helmholtz free energy. Besides this, at equilibrium, three other requirements must be satisfied: $\nabla\mu(\mathbf{r}) = 0$, $\nabla \cdot \mathbf{p} = 0$, and $\nabla T(\mathbf{r}) = 0$. The first condition states that the chemical potential μ must be the same in all points in the system, given that particles can diffuse (i.e., it is a homogeneous property).[53] The second one is called the condition of mechanical equilibrium, which says that the divergence of the pressure tensor $\mathbf{p}$ is the null vector. Thus, the mechanical equilibrium condition does not require that the pressure is homogeneous (indeed, the pressure is not homogeneous in the system having a curved interface).[54] The third is similar to the first one but for T. In the Gibbsian formulation of curved interfaces, one assumes that the system is composed of two macroscopic phases divided by a surface of zero volume.[55] The properties of each of these macroscopic phases (p, density ρ, and μ) are obtained from the properties of a bulk system. Therefore, the Gibbsian picture is that one has two bulk phases separated by an interface. Although the interface has zero volume, it contributes to the thermodynamic properties of the system (except for volume). The number of molecules at the interface, also known as excess particles N_{exc}, can be obtained from the equations

$$N = N_{sol} + N_L + N_{exc} = \rho_{sol} V_{sol} + \rho_L V_L + N_{exc}, \tag{1}$$

$$V = V_{sol} + V_L, \tag{2}$$

where the subscript *sol* denotes the properties of the solid and the subscript L denotes the properties of the external liquid phase. One then writes the Helmholtz free energy of the system F as

$$F = N_{sol}\mu_{sol} - p_{sol}V_{sol} + N_L\mu_L - p_L V_L + N_{exc}\mu_{exc} + \gamma A_{sol}, \tag{3}$$

where A_{sol} is the area of the interface and γ is the interfacial free energy. Strictly speaking, a thermodynamic description is only possible when the system is at equilibrium. There, μ is homogeneous so that we can write that $\mu_{sol} = \mu_L = \mu_{exc} = \mu$, where μ_{exc} is the chemical potential of the excess particles (not to be confused with the excess chemical potential used in statistical mechanics), and F can be written as

$$F = N\mu - p_{sol}^{\mu} V_{sol} - p_L V_L + \gamma A_{sol}. \tag{4}$$

The meaning of the superscript μ in the pressure of the solid will be clarified later on. By writing explicitly the dependence of the volume and area on the radius of the spherical solid cluster, one has

$$F = N\mu - p_{sol}^{\mu}\left(4/3\pi R_{sol}^3\right) - p_L\left(V - 4/3\pi R_{sol}^3\right) + \gamma\left(4\pi R_{sol}^2\right). \tag{5}$$

At a molecular scale, there is some arbitrariness in determining R_{sol}. Since F, μ, p_{sol}^{μ}, and p_L are fixed, changing R_{sol} for a certain system also changes the value of γ. There are two popular choices for R_{sol}. The first is the Gibbs dividing surface, $R_{sol} = R_{sol}^e$, for which the number of excess particles N_{exc} is zero (meaning that particles belong either to the solid or to the liquid, but not to the interfacial region). The second is the surface of tension, $R_{sol} = R_{sol}^s$, for which γ is a minimum with respect to changes in the location of the dividing surface (γ^s). Actually, by taking the notational derivative (i.e., an arbitrary change in R_{sol} without any physical change in the system) represented by square brackets, one obtains

$$p_{sol}^{\mu} - p_L = 2\frac{\gamma}{R_{sol}} + \left[\frac{d\gamma}{dR_{sol}}\right]. \tag{6}$$

By definition, $[d\gamma/dR_{sol}] = 0$ when $R_{sol} = R^s_{sol}$, leading to the celebrated Young–Laplace equation

$$p^{\mu}_{sol} - p_L = 2\frac{\gamma^s}{R^s_{sol}}. \tag{7}$$

One difficulty in dealing with crystal–melt interfaces arises from the crystals ability to support elastic stress. What is the value of the pressure of the internal phase to be used in the thermodynamic description? We have shown recently that, for HS, the actual pressure of the solid cluster is smaller than that of the external liquid[56] (this observation had been also made in a Lennard-Jones system[14]). That would lead to a negative value of γ^s which is unphysical. As a matter of fact, since solids can support stress, its actual pressure is related to the external pressure and the curvature toward a similar relation to that of Eq. (7) albeit somehow different since it is found from mechanical arguments instead of thermodynamical. In this case, $p_{sol} - p_L = 2f/R$, where f is the surface stress and R is the mechanical radius of the solid.[57–59] We mentioned previously that μ is homogeneous in the system so that it is the same in the liquid and in the solid phase. However, the actual pressure leads to a value of μ for the bulk solid phase, which is different from that of the liquid phase spoiling completely the thermodynamic treatment. Therefore, since we know for sure that μ is homogeneous, we should use the value of the pressure of a "bulk" solid phase with the same μ as the external liquid phase. That explains the origin of the superscript μ in the pressure of the solid. Implicitly, this shows that the critical nucleus presents subtle differences with respect to a bulk phase. In a sense, the thermodynamic description of spherical solid phases requires the properties of a "virtual" solid rather than the properties of the actual solid. The use of virtual states as reference states is common in thermodynamics. It is used, for instance, in binary mixtures for defining the reference state of the solute (in the assymetric criteria).[60] Therefore, for p_{sol} and ρ_{sol}, one should use the values of a virtual bulk solid having the same μ as that of the external liquid phase. This argument was already suggested by Tolman (although in a different context),[61] introduced theoretically in the paper of 1984 by Mullins[52] followed later by Cacciuto *et al.*,[62,63] and has been proven to be correct in our recent work.[56] As a matter of fact, Gibbs clearly stated that one should consider the properties of a bulk phase.[55] The solid cluster has stress and does not behave as a bulk phase. Indeed, Richard and Speck observed a smoothly decaying average density profile with a density at the center of the nucleus that was smaller than the bulk density at the same μ.[13] This was also observed in Ref. 56. Nevertheless, since in this formalism one uses bulk properties, there is no need to know the actual properties of the solid cluster.

Moreover, there are some useful relations that hold when the system is at equilibrium. One of these relates γ^e (the value of the interfacial free energy when one uses the Gibbs dividing surface R^e_{sol}) and γ^s,

$$\gamma^e = \gamma^s\left[\frac{(R^s_{sol})^n + (n-1)(R^e_{sol})^n}{nR^s_{sol}(R^e_{sol})^{n-1}}\right]. \tag{8}$$

The relation between γ^s and γ^e for a spherical interface was known from previous work.[20] Here, we extend it (rigorously) to three interfaces (sphere, cylinder, or planar). The value of n in the previous equation can be $3, 2, 1$, which corresponds to a spherical, cylindrical, or planar interface respectively. Note that γ^e is larger than γ^s for the sphere and the cylinder as γ^s, by definition, is the value of γ at the minimum, which defines the surface of tension R^s_{sol}. The previous equation is found from the generalization[64,65] of Eq. (7), which is given by

$$p^{\mu}_{sol} - p_L = (n-1)\frac{\gamma^s}{R^s_{sol}}. \tag{9}$$

At this point, we would like to make a comment for the planar interface. When one has a planar interface at equilibrium, there is no difference in pressure between the solid and the liquid phase so that in this case, $p_{sol} = p_L$. In addition, for a planar interface R^e_{sol} is well defined but R^s_{sol} is not. In fact, since for a planar interface the value of A does not change by moving the location of the interface, the value of γ is invariant to changes in the location of the interface, and there is no minimum of γ as a function of the location of the dividing surface, which is the property that defines R^s_{sol}. Of course, for a curved interface, there is always a difference between R^e_{sol} and R^s_{sol} for arbitrarily large solid clusters, but the distance between these two surfaces at a planar interface is a wrong concept. One could, of course, talk about the limit to infinite size of the distance between R^e_{sol} and R^s_{sol}, which is the definition of the Tolman length δ_T, an important parameter to explain the curvature dependence of the interfacial free energy.[1,6,10,35,61] Thus, for a planar interface, γ does not depend on the dividing surface, and in this case, the Gibbs dividing surface is the most convenient choice.

Now, the reader may get the feeling that evaluating γ is a simple task. In fact, if F were known, one assigns a value to R_{sol}, and since all terms in Eq. (5) are known but γ, one then obtains a value for the interfacial free energy γ. By using different values for R_{sol}, one could easily obtain the one for which γ is a minimum, thus finding γ^s and R^s_{sol}. Nevertheless, the value of F for the inhomogeneous system having the curved interface is, in general, unknown both in experiments and in computer simulations so that our knowledge of γ for curved interfaces is limited or absent. We have a rigorous formalism which is difficult to apply. Furthermore, in general, there is no rigorous mechanical route to γ (i.e., obtaining γ from the pressure tensor).[7,9,59,66–68] The only exception to this rule is the case of a planar interface between two fluid phases at coexistence.[69,70] Not surprisingly, hundreds of papers present results of γ (both from experiments and from simulations) for the planar interface between two fluid phases at equilibrium, but results for γ for curved fluid–fluid interfaces or for solid–fluid interfaces at equilibrium are scarce.

However, as we have shown recently, the stable spherical solid cluster at constant N, V, and T is critical in the NpT ensemble, and since nucleation rates J (which can be measured in the laboratory) can be described quite well by classical nucleation theory (CNT, as described by the Volmer–Weber–Becker–Doring–formalism[71–85]), the values of γ^s obtained by fitting nucleation rates to CNT could also be used in the thermodynamic description of the system at equilibrium in the NVT. Turnbull was the first to realize that nucleation studies could be useful to learn something about the value of γ,[73] and it is fair to recognize that only recently have we been able to understand the connection properly. When using CNT, one is using R^s_{sol} and γ^s as the Young–Laplace equation is implicit in the formalism, which leads to the key equations of CNT (see Appendix A). We have shown that the values of γ^s obtained from nucleation studies allow

one to describe the equilibrium case. An important result of these previous studies performed in our group is that now we know how the value of γ^s changes with the physical changes in R^s_{sol}.[35,48] In fact, we found that Tolman's equation

$$\gamma^s = \gamma^0\left(1 - 2\frac{\delta_T}{R^s_{sol}}\right), \tag{10}$$

with parameters $\delta_T = -0.41\sigma$ and $\gamma^0 = 0.576\ \mathrm{kT}/\sigma^2$, where σ represents the hard sphere diameter, describes quite well the value of γ^s for HS. Note that for γ^0 we use an average value of γ from planar interfaces at equilibrium having low Miller indices. Although our previous studies deal with the spherical interface, Eq. (10) can be extended to cylinders as follows:

$$\gamma^s = \gamma^0\left(1 - \frac{\delta_T}{R^s_{sol}}\right). \tag{11}$$

Note that we use the same δ_T for cylinders although certainly this is not necessarily true. Nevertheless, as shown in Ref. 86, the difference between δ_T of the spherical geometry differs only slightly from the one for cylinders so it seems to be a reasonable approximation. For a planar interface, we shall use $\gamma^s = \gamma^0$, although a planar interface has certain Miller indices given by *hkl*, so that the value of γ^0, which is an average of several planes, is only an approximation, and one should use the value of γ of the actual plane exposed to the liquid. Furthermore, from our previous studies[35] of HS, we learned about the distance between the radius R^e_{sol} and R^s_{sol}. We found that the distance between these two important surfaces is not constant but it changes with the radius as

$$R^e_{sol} - R^s_{sol} = \delta_T + 2.613\sigma^2/R^s_{sol}. \tag{12}$$

Therefore, one can state that for hard spheres, we have a detailed description of the curved interface between a spherical solid cluster and a liquid phase at equilibrium that can easily be extended to cylindrical and planar solid clusters as well.

III. THERMODYNAMICS OF CURVED INTERFACES: EXTENSION TO CONFIGURATIONS FAR FROM EQUILIBRIUM

The main purpose of this work is to propose an approximate treatment which describes not only the Helmholtz free energy F in a NVT system at equilibrium but also the free energy profile within the NVT ensemble as a function of a certain order parameter. The natural choice of the order parameter for the system considered in this work, a system of hard spheres in the NVT ensemble at high densities, is the size of the solid cluster N_S. When there is no solid cluster, the system is a homogeneous liquid. By changing N_S, we can determine the free energy profile, i.e., how the value of F changes with the order parameter. Note that we use the subscript *sol* when the solid is in stable equilibrium with the liquid and the subscript S when this is not the case. Thermodynamics describes the average properties of a system which are obtained mainly from configurations within 10–15 kT to the minima of the free energy profile. Thermodynamics cannot provide information about the probability of obtaining particular configurations far away from the typical ones close to the minimum (these configurations will have little probability). Therefore, strictly speaking, thermodynamics reasoning cannot provide a free energy profile. If one is interested in a rigorous description of the free energy profile (which describes the probability of configurations far away from the average value of the order parameter), then statistical mechanics should be used (see Appendix B). Therefore, any treatment with a "thermodynamic" flavor aimed at obtaining the free energy profile from thermodynamic arguments must be necessarily approximate. We will present here a treatment of this type. With the right input, the treatment should correctly describe the properties of the system when close to local minima, but it will be only approximate for configurations far away from this minima.

The basic idea of the approach is to write F as in Eq. (5) but allowing μ_S and μ_L to be different. This expression introduces a problem as now one must define μ_{exc} which is unknown, but this problem can be formally removed by adopting the Gibbs dividing surface which we shall denote as R^e_S. Then,

$$\begin{aligned} F\left(R^e_S\right) = {} & \rho_S\left(4/3\pi\left(R^e_S\right)^3\right)\mu_S - p_S 4/3\pi\left(R^e_S\right)^3 \\ & + \rho_L\left(V - 4/3\pi\left(R^e_S\right)^3\right)\mu_L - p_L\left(V - 4/3\pi\left(R^e_S\right)^3\right) \\ & + \gamma_e\left(R^e_S\right)\left(4\pi\left(R^e_S\right)^2\right). \end{aligned} \tag{13}$$

We use this expression as the one describing the free energy profile. In the supplementary material, it is a FORTRAN program with comments that allows one to compute the free energy profile. In the scheme, first, we shall define the total number of particles in the system N, the volume of the system V, and the geometry we want to consider (given by n). Then, in order to obtain the values of the variables $\rho_S, p_S, \mu_S, \rho_L, p_L, \mu_L$, and $\gamma_e(R^e_S)$ for a certain value of R^e_S, we follow these simple assumptions and calculation steps:

Assumption 1 (considering bulk phases). We assume that both the solid cluster and the liquid are bulk phases. That means that we only need one of the variables ρ, p, μ to determine the other two. In fact, ρ and p are connected through the equation of state (EOS), and μ can be obtained from the expression

$$\mu = \int_{p_{coex}}^{p} \frac{1}{\rho(p)}\,dp, \tag{14}$$

where p_{coex} is the pressure at which a bulk solid and a bulk liquid have the same chemical potential μ and also where both phases will coexist when having a planar interface. For practical convenience, we will set $\mu_S(p_{coex}) = \mu_L(p_{coex}) = 0$. For the pseudo-HS potential, we have shown using computer simulations that $p_{coex} = p/(kT/\sigma^3) = 11.648$ (very close to the value of true HS which is around 11.57[87–89]). This value is used in the scheme. In addition, in the calculation, we use the bulk EOS computed in simulations. A figure can be found in the supplementary material of Ref. 56 as well as the parameters of the fit that are also included in the program provided in the supplementary material of this work. The EOS can also be seen in the caption of Table II.

Assumption 2. (applying equilibrium equations). We assume that all the equations we found for the stable solid cluster also hold for configurations with little probability (i.e., configurations where the value of the order parameter is far away from the average value

TABLE II. Parameters for the theoretical scheme. Along with these parameters, one has to define also the values of N and V. Furthermore, the following EOS (in reduced units) are used: for the solid $p_{sol} = 162.96\rho_{sol}^2 - 299.42\rho_{sol} + 146.8$, and for the liquid $p_L = 141.04\rho_L^2 - 212.12\rho_L + 86.29$. Reduced units for pressure are given by (kT/σ^3) and for density by (σ^{-3}).

n	$\gamma^0/(kT/\sigma^2)$	δ_T/σ	$p_{coex}/(kT/\sigma^3)$
Sphere: 3 Cylinder: 2 Planar: 1	0.576	−0.41	11.648

at equilibrium). Although these configurations appear via fluctuations at equilibrium, from the point of view of thermodynamics, these look like non-equilibrium configurations as they are far away from the average value of the order parameter of the system at equilibrium. Therefore, we shall assume that the equations that are valid to describe the system in the proximities of the minimum in the free energy (i.e., when N_S is close to N_{sol}) can also be used for configurations where N_S is significantly different from N_{sol}.

In particular, we shall assume that the distance between R_S^e and R_S^s is given by Eq. (12), that the value of $\gamma^s(R_S^s)$ can be taken from the generalized Tolman's equation [Eq. (10) in the case of spherical solid clusters], that $\gamma^s(R_S^s)$ and $\gamma^e(R_{sol}^e)$ are related via Eq. (8), and that the generalized Young–Laplace equation [Eq. (9)] describes the difference in pressure for these values of $\gamma^s(R_S^s)$ and R_S^s. Therefore, the values of δ_T and γ^0 have to be provided.

Step 1: Estimating $\gamma^e(R_S^e)$

A radius at the surface of tension is selected, R_S^s, and its corresponding equimolar dividing surface R_S^e is found from Eq. (12). Then, the interfacial free energy at the surface of tension, $\gamma_s(R_S^s)$, is found from Eq. (10) for a spherical nucleus or Eq. (11) for a cylinder. We use γ^0 as a good approximation for the planar interface. Once one knows $\gamma_s(R_S^s)$, by using Eq. (8), one obtains $\gamma_e(R_S^e)$.

Step 2: Determining p_S, ρ_S, p_L, and ρ_L

A trial value is used for p_L, which, in turn, gives the corresponding ρ_L via the EOS that is provided. Then, since we already know $\gamma_s(R_S^s)$ and R_S^s, by using Eq. (9) for this trial p_L, we obtain p_S. Once we have p_S, we use the EOS to find ρ_S. Now, whether this trial is valid or not depends on the equation

$$N = \rho_S 4/3\pi\left(R_S^e\right)^3 + \rho_L\left(V - 4/3\pi\left(R_S^e\right)^3\right). \tag{15}$$

We drop the superindex μ in p_S although we consider bulk properties because in this case, the chemical potential of the solid cluster is different from that of the liquid. The left side of the equation is known; by computing the right side for trial values of p_L, one can find the value that fulfill Eq. (15). Then, for this value, one obtain F with Eq. (13) and returns to Step 1 to select another value of the radius of tension.

In short, the approximate treatment proposed in this work uses relations that are rigorous for the equilibrium solid cluster for any value of N_S although allowing μ to be different among phases. The reader should not look to our treatment as a rigorous thermodynamic treatment. The only way to obtain $F(N_S)$ rigorously is by means of the statistical mechanics formalism (see Appendix B). However, this formalism may be useful if it is capable of theoretically explaining the size of the stable solid clusters found in our simulation studies and to describe qualitatively the free energy curve. Theory is faster than simulation, and besides, it can be useful to determine any set of thermodynamic conditions under which the solid clusters are stable. We can implement the theory for a spherical solid cluster ($n = 3$), for a cylindrical solid cluster ($n = 2$), or for a planar interface ($n = 1$).

IV. RESULTS

In a previous work, we studied ten spherical solid clusters of hard spheres surrounded by liquid, which were stable/metastable in the NVT ensemble.[35] The parameters for the system in which those solid clusters where stabilized as well as the size of the solid clusters can be found in Table I. We performed molecular dynamics simulations of pseudo-HS in the GROMACS package. The continuous potential that almost reproduces HS was proposed by Jover *et al.*,[44] and it is given by the expression

$$U_{PHS}(r) = \begin{cases} 50\left(\frac{50}{49}\right)^{49}\epsilon\left[\left(\frac{\sigma}{r}\right)^{50} - \left(\frac{\sigma}{r}\right)^{49}\right] + \epsilon, & r < \left(\frac{50}{49}\right)\sigma, \\ 0, & r \geq \left(\frac{50}{49}\right)\sigma, \end{cases} \tag{16}$$

where σ represents the hard sphere diameter and ϵ is the depth of the potential. This potential mimics the properties of HS when the reduced temperature is $T/(\epsilon/k) = 1.5$ (although, for true HS, T is not relevant). In this paper, we use reduced units so that the length is given in units of σ, density in units of σ^{-3}, pressure in units of kT/σ^3, and chemical potential in kT units. When implementing the theory described before, instead of presenting the value of F, we subtract the free energy of a homogeneous liquid phase at the conditions given by N and V. We shall use the superscript "o" for it,

$$F^o = N\mu_L^o - p_L^o V. \tag{17}$$

Thus, we shall define ΔF as

$$\Delta F(N_S) = F(N_S) - F^o. \tag{18}$$

At the end of the calculations, one has for a certain value of N and V, the free energy curve ΔF as a function of the size of a spherical, cylindrical, or planar solid cluster. The local minimum in ΔF corresponds to stable solid clusters although it may not correspond to the absolute minimum in ΔF so that they may be only metastable. In a local minimum, ΔF is negative/positive when the considered solid cluster is more/less stable than the homogeneous liquid. Let us first present the results obtained in the theoretical treatment for system I, which is characterized by $N = 10\,540$ and $V = 10\,686.4\sigma^3$. This is shown in Fig. 2(a).

As can be seen, the spherical solid cluster is less stable than the homogeneous liquid (i.e., ΔF is positive in that minimum). There is a free energy barrier separating the homogeneous liquid from the spherical solid cluster, $\Delta F_{sol}^{unstable}$. Therefore, both transitions, from liquid into a spherical solid cluster surrounded by liquid and from such a system into the homogeneous liquid, are activated processes. The size of the solid cluster at the maximum is around 500 particles. That means that if one introduces a larger spherical solid cluster

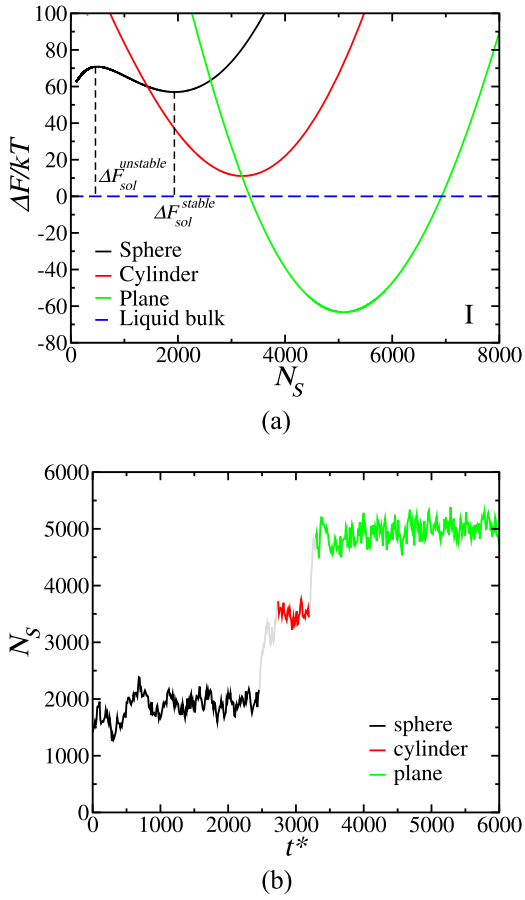

FIG. 2. Both panels correspond to system I (i.e., $N = 10\,540$ and $V = 10\,686.4\sigma^3$). (a) Free energy profiles as a function of N_S. Results are shown for spherical (black), cylindrical (red), and planar solid clusters (green). These profiles should go to zero at $N_S = 0$, but we start the calculation from a certain size to avoid numerical issues. (b) Simulation results for the evolution of the solid cluster number of particles over time. The simulation starts from a configuration having a spherical seed surrounded by liquid. The shape of the solid cluster transits from spherical to cylindrical and then to planar. Time is in reduced units $t^* = t/\tau$ where $\tau = \sigma\sqrt{m/(kT)}$ is the unit time. This time unit is in the order of two diffusive times computed as the time required for a particle to diffuse further than its size.

in a liquid while the system fulfills $N = 10\,540$ and $V = 10\,686.4\sigma^3$, the solid cluster will grow at the expense of the liquid following a downhill trajectory in the free energy profile, $\Delta F(N_S)$, to reach the size of the metastable spherical solid cluster. An example of that can be found in Fig. 2 of our previous work (for system IX).[35] The solid cluster at the maximum is a critical nucleus (in the NVT ensemble) as shown in the seeding study performed by Richard and Speck.[13] The cylindrical solid cluster is more stable than the spherical one (although still less stable than the homogeneous liquid). The planar solid cluster is the absolute minimum in ΔF. The homogeneous liquid phase, the spherical and cylindrical solid clusters are just metastable states of the system. Thus, in the phase coexistence diagrams developed by Binder and co-workers, system I is within the planar region. Further work on the phase coexistence diagram will follow afterward. In our simulations of system I [see Fig. 2(b) where the size of the nucleus over time is shown], we found that the spherical solid cluster was stable for a few thousand diffusive times. However, at a certain point, a fluctuation occurred and the system transformed into the cylindrical solid cluster. That makes sense as the cylindrical solid cluster is more stable than the spherical one. It also means that the conversion from the spherical solid cluster into a cylindrical solid cluster is an activated process and one must overcome a free energy barrier. The theoretical treatment of this work considers the transformation of a homogeneous liquid into a spherical, cylindrical, or planar solid cluster surrounded by liquid, but not the transformation between the sphere and the cylinder or between the cylinder and the planar slab surrounded by liquid. In this work, we have simulated the homogeneous liquid for very long times, and it never transformed into the spherical solid cluster surrounded by liquid, which makes sense as the free energy barrier is of about 70 kT. However, we also simulated the stable cylinder and we could observe how it transformed into the planar interface easily, thus indicating that there is only a small free energy barrier separating the two states. The free energy curve transforming a homogeneous liquid directly into a planar interface has a huge free energy barrier. Hence, the way the system should reach the global equilibrium is by using several steps, i.e., transforming first the homogeneous liquid into a spherical solid cluster surrounded by liquid (with a free energy barrier of 70 kT), then the spherical solid cluster into a cylindrical one, and finally the cylinder into the planar slab. To the best of our knowledge, this is one of the first examples of a complex mechanism for nucleation to reach the global equilibrium state.

The theory is quite successful in predicting the size of the metastable spherical and cylindrical, and the size of the stable planar solid clusters. In the spherical case, for instance, the local minimum of ΔF occurs for about 1941 particles to be compared with the simulation results, which was 1925(100). In the cylindrical case, we theoretically obtain 3200 for 3400(100) in the simulation, and in the planar one, we get 5090 for 5015(100) in the simulation. The value in parentheses is the estimated error, as in simulations the spherical solid cluster presents capillarity fluctuations, and one must determine its average size along the run. In this calculation, we used a value of γ for a planar interface (i.e., at $p = p_{coex}$), which is the average of several planes. However, for a planar solid–liquid interface of hard spheres, γ has about 10% of anisotropy depending on the exposed plane.[90] Since the interfacial free energy of a curved interface is obtained using Tolman's equation with $\gamma^0 = 0.576\ kT/\sigma^2$ and $\delta_T = -0.41\sigma$, if one uses a different value of γ^0, another value of δ_T should be used as well. Note that the nucleation results that were used to obtain such Tolman length extrapolate very close to $0.576\ kT/\sigma^2$. The possibility to extend this study toward nuclei with facets where the anisotropy in γ is unavoidable is beyond the scope of this work, although it represents a very interesting possibility for future work. Thus, the theoretical treatment of this work is able to provide a coherent picture of the free energy profile of the system and to reproduce simulation results. The only weak point is that we are missing the possibility to describe the transformation of sphere → cylinder → plane as the intermediate state in this transitions would have a complex intermediate geometry that would require a more elaborated treatment.[43] Note that the crossing of two solid curves (for instance, for the sphere and cylinder) in Fig. 2 is not

particularly useful as it only indicates that a spherical and a cylindrical solid cluster with the same number of particles have the same free energy with respect to the homogeneous liquid. Unfortunately, when the crossing occurs, the pressures of the corresponding liquids and their chemical potentials are different so that the crossing is not a transition state.

Let us now present the results for other systems. This is done in Fig. 3 for six of the ten systems considered in our previous work

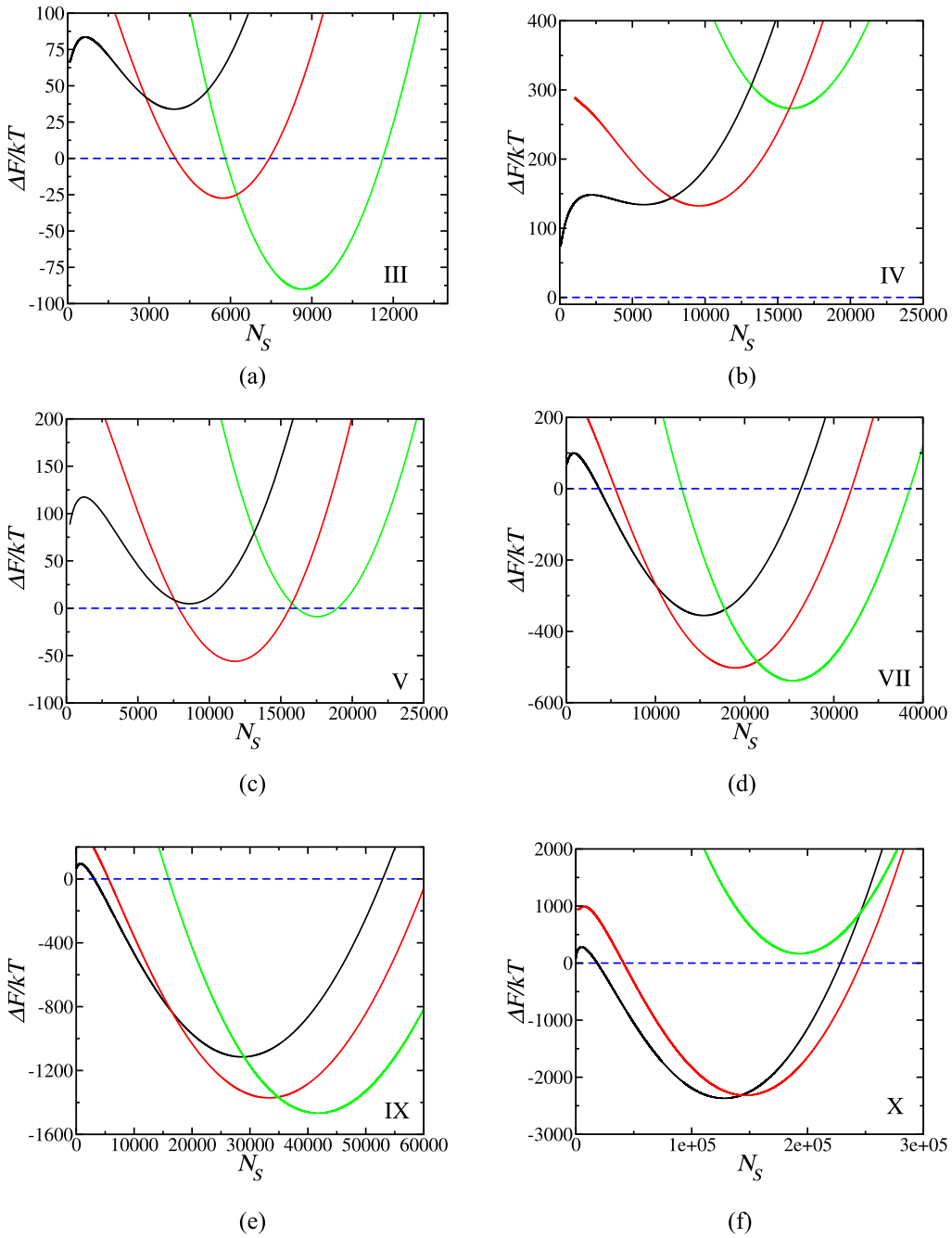

FIG. 3. Approximate free energy profile for the formation of a spherical (black), cylindrical (red), or planar (green) solid cluster from a metastable liquid in a HS system for systems (a) III, (b) IV, (c) V, (d) VII, (e) IX, and (f) X. We keep the same labels as in our previous simulation work.[35] The corresponding parameters of the system size N and volume V can be seen in Table I following the label in the bottom-right corner of each panel within this figure, the resulting stable size is shown and compared with simulations in Table III, and the estimated pressures and densities are shown in Table IV.

(III, IV, V, VII, IX, and X). Apart from those that are plotted, for systems II, VI, and VIII, we obtained liquid as the global minimum for the first two and cylinder for the last one. We can make the following interesting observations:

- In general, the spherical interface is rarely the global equilibrium state of the system. System X is the only exception for the considered cases.
- A jump from sphere to cylinder was found in simulations in our previous work for systems, I, III, and IX. In fact, the theoretical treatment predicts that the cylindrical solid cluster is more stable than the spherical one. For systems IV and X, it is clear that this jump to the cylinder should not occur as the cylinder is less stable than the sphere. However, for system VII, this jump is possible although not observed in our simulations.
- The homogeneous liquid is the most stable state for systems II, IV, and, VI (note that systems II and VI are not shown). In case IV, for instance, the pressure of the homogeneous liquid is $p = 13.35\ \mathrm{kT}/\sigma^3$, which is significantly higher than the pressure at which the solid and liquid coexist via a planar interface, $p_{coex} = 11.648\ \mathrm{kT}/\sigma^3$. Even though the pressure is higher than the pressure at planar coexistence, the liquid is more stable on its own than surrounding a spherical, cylindrical, or planar solid cluster. Thus, one has achieved a "superstabilizaton" of the homogeneous liquid.[91,92] There, the homogeneous liquid becomes the stable thermodynamic phase.

In Fig. 4, we present the difference in chemical potential between the two phases $\Delta\mu = \mu_S(p_S) - \mu_L(p_L)$ as a function of N_S for the spherical shape in system VII. Since we set the Young–Laplace equation as true for any N_S, the derivative of ΔF, i.e., $d\Delta F/dN_S$, is given by $\Delta\mu$. In practice, a surface term may slightly affect the slope of ΔF, given that our treatment might fail to exactly fulfill the interfacial Gibbs–Duhem relation, which is given by[20] $[d\gamma/dR]_{R=R_e} = (\partial\gamma^e/\partial R^e)_T$ (this problem does not arises if the capillarity approximation is used, i.e., $\gamma^e = \gamma^s = \gamma_{coex}$, but this is against the evidence found in the last three decades that γ is not constant and changes with the curvature of the interface). In any case, the difference between $\Delta\mu$ and $d\Delta F/dN_S$ (obtained from finite differences) although not zero (as it should be when the interfacial Gibbs–Duhem relation is satisfied exactly) is very small. As expected, $\Delta\mu$ vanishes at the values of N_S corresponding to the extrema of ΔF. The first value of N_S where $\Delta\mu = 0$ corresponds to the maximum in ΔF. This is a critical nucleus in the NVT ensemble. It is an unstable equilibrium as the chemical potentials of both phases are the same, but it is in a maximum of ΔF. The second value of N_S where $\Delta\mu = 0$ corresponds to the minimum in ΔF so that it corresponds to a stable or metastable equilibrium (depending on whether the local minimum is also the global minimum). This is also a critical nucleus (in the NpT ensemble), but it is stable at the same time (in the NVT ensemble). Thus, at equilibrium, the chemical potential of both phases are the same.

In Fig. 5, the value of the pressure of the liquid phase obtained from the theoretical treatment is presented as a function of the curvature $1/R_s^s$ of the spherical solid cluster for systems I, III, IV, and X. Along with these results, we show a fit to NVT-seeding results from Ref. 35. As can be seen, there are two crossing points between the fit and each system curve, one corresponding to a maximum in ΔF and the other to the minimum. At some point, when the solid cluster is large enough, liquid pressure abruptly goes down as the crystalline phase is of higher density.

Now, by taking the values of the solid cluster size at the minima of ΔF, i.e., $N_S = N_{sol}$, we can compare with our computer simulation results from previous work.[35] As shown in Table III, our approach gives results for the spherical geometry that agree very well with the simulations. The deviation is in average below 2.5% for the nucleus size N_{sol} and below 0.8% for its radius R^s_{sol}. The error tends to be higher for small systems. Thus, the theoretical treatment is able to

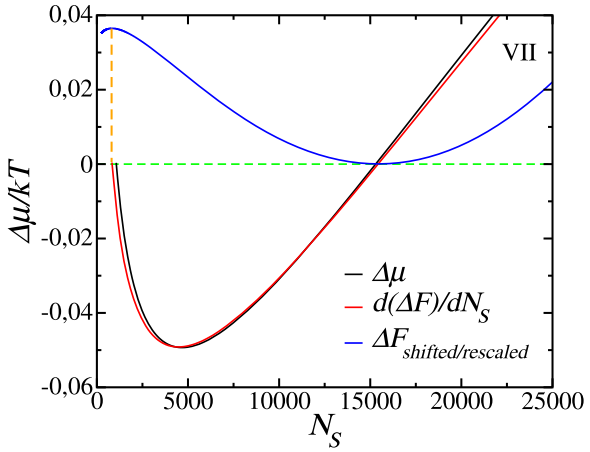

FIG. 4. In black, we show the chemical potential difference $\Delta\mu = \mu_S - \mu_L$ (in kT units) and in red, the derivative of ΔF both as a function of N_S. Results are for system VII. The derivative is obtained from finite differences. When $\Delta\mu = 0$, then ΔF approaches an extremum in accordance with Fig. 3(d). In blue, we show a rescaled ΔF to demonstrate that the minimum of ΔF corresponds to the second root of $\Delta\mu$. On the other hand, the first root corresponds to the maximum in ΔF (see the vertical line).

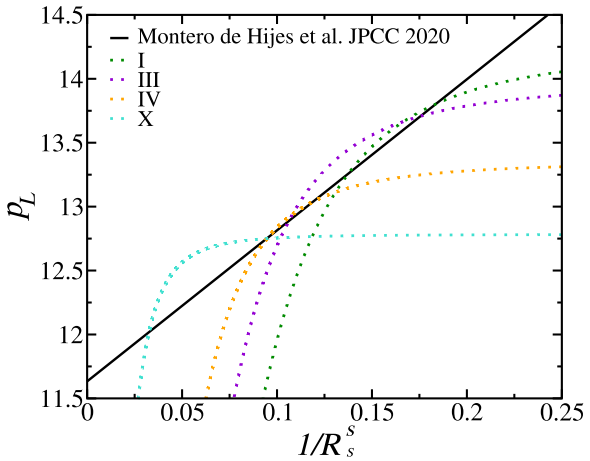

FIG. 5. Pressure in the liquid phase is represented against the inverse of the radius of the solid cluster for systems I, III, IV, and X. The solid line is a fit to data from Ref. 35.

TABLE III. Tabular comparison of spherical solid clusters in simulation[35] and theory for different thermodynamic conditions obtained from the minimum of ΔF. In addition, deviations of theoretical estimations with respect to the simulation values are presented $\Delta N_{sol} = (|\langle N_{sol}^{sim}\rangle - N_{sol}^{theory}|)/\langle N_{sol}^{sim}\rangle$ and $\Delta R_{sol}^{s} = (|\langle R_{sol}^{s,sim}\rangle - R_{sol}^{s,theory}|)/\langle R_{sol}^{s,sim}\rangle$. In addition, uncertainty in $\langle N_{sol}^{sim}\rangle$ were estimated from the standard deviation of block averages in simulations, whereas in the theoretical approach, they were obtained from error propagation (the brackets stands for the average as in simulations N_{sol} has capillary fluctuations). In all cases, uncertainties were in the range of 1%–5% so that they are comparable with the deviations. We use reduced units for distance (σ) and volume (σ^3). The parameters of the NVT system can be seen in Table I.

Label	$\langle N_{sol}^{sim}\rangle$	N_{sol}^{theory}	ΔN_{sol} (%)	$\langle R_{sol}^{s,sim}\rangle$	$R_{sol}^{s,theory}$	ΔR_{sol}^{s} (%)
I	1 925	1 941	0.8	7.54	7.55	0.1
II	2 736	2 952	7.9	8.48	8.70	2.6
III	3 718	3 926	5.6	9.40	9.57	1.8
IV	5 604	5 783	3.2	10.79	10.90	1.0
V	8 602	8 614	0.1	12.46	12.46	0.0
VI	10 498	10 770	2.6	13.32	13.43	0.8
VII	15 554	15 427	0.8	15.20	15.15	0.3
VIII	23 558	23 419	0.6	17.47	17.43	0.2
IX	28 879	28 616	0.9	18.70	18.64	0.3
X	129 926	127 891	1.6	30.93	30.75	0.6

describe quite well the size of the spherical solid clusters obtained in simulation. Let us now compare the theoretical predictions for the cylindrical and planar geometry. For systems III and IX, we theoretically estimate stable cylinders of 5720 and 33 240 particles, respectively. In simulations, we found in our previous work that the sizes for these systems are 5800 and 34 150 particles, i.e., about 2.5% deviation. Regarding the planar slab, we perform a new simulation of a planar slab in stable equilibrium in a system of 15 800 particles and $16\,000\sigma^3$ volume. In this simulation, the planar solid cluster has 8300 particles, while our theoretical calculation estimates have 7836 particles so that we had about 5.5% difference. Since the length of the simulation box does not necessarily match an integer number of times the length of the unit cell, it is reasonable that the solid is under some stress, which is not included in our theoretical treatment. Besides the value of γ^0 used in this work is the average of the interfacial free energy for several planar interfaces, but, of course, when introducing only a plane, the value of this plane should be used. In any case, the prediction is quite reasonable even for the planar interface.

At this point, we compare the pressures and densities with those at the simulations. For the simulation results, we shall use the pressure p_{sol}^{μ} that a perfect solid bulk would have at the same μ as the liquid and not its actual pressure. To do so, we first obtain the chemical potential the liquid from its pressure (obtained from its density and the EOS) by means of Eq. (14), and then, we use that value of μ to obtain the pressure of the solid with the help of the EOS of the solid (the same than in the theoretical approach). As shown in Table IV, this theoretical treatment with a few simulation inputs reproduces almost exactly the simulation results.

As we mentioned before, the stable/metastable spherical solid clusters found in the NVT become critical when one performs simulations in the NpT ensemble (using the same value of N and with

TABLE IV. Tabular comparison of pressure and density of spherical solid clusters and surrounding liquid in simulation[35] and theory for different thermodynamic conditions obtained from the minimum of ΔF. Deviations are in all cases smaller than 1%. We use reduced units for pressure (kT/σ^3).

Label	$p_{sol}^{\mu,sim}$	p_{sol}^{theory}	$\rho_{sol}^{\mu,sim}$	ρ_{sol}^{theory}	p_{L}^{sim}	p_{L}^{theory}	ρ_{L}^{sim}	ρ_{L}^{theory}
I	13.38	13.32	1.078	1.076	13.21	13.15	0.970	0.969
II	13.18	13.13	1.074	1.073	13.03	12.96	0.967	0.966
III	13.03	12.98	1.071	1.070	12.89	12.85	0.964	0.964
IV	12.86	12.82	1.067	1.066	12.74	12.70	0.962	0.961
V	12.68	12.66	1.063	1.063	12.58	12.56	0.959	0.959
VI	12.61	12.58	1.062	1.061	12.52	12.49	0.958	0.957
VII	12.48	12.47	1.059	1.059	12.40	12.39	0.956	0.956
VIII	12.37	12.35	1.056	1.056	12.31	12.29	0.954	0.954
IX	12.32	12.31	1.055	1.055	12.26	12.24	0.953	0.953
X	12.05	12.03	1.049	1.049	12.01	11.99	0.949	0.949

$p = p_L$). This connection allows us to obtain extra information from the local minima of ΔF, as they are critical nuclei in the NpT ensemble. Therefore, one can estimate the free energy barrier ΔG_{sol} (i.e., the maximum in the Gibbs free energy change when the critical nucleus is formed from a homogeneous liquid while keeping N, p, and T constant, which was denoted as ΔG_c in our previous works[35]). At the minimum of ΔF, we can compute the Gibbs free energy barrier corresponding to nucleation through an isobaric–isothermal path (at $p = p_L$) simply as $\Delta G_{sol} = A(R_{sol}^{s})\gamma^{s}/3$. See Appendix A for more details. In Fig. 6(a), we present these calculations along with previous molecular dynamics results.[78,82] As can be seen, this theoretical description reproduces the simulation results for free energy barriers to nucleation ΔG_{sol}. In Fig. 6(b), we show the dependence of the liquid pressure at which a certain nucleus is critical against its critical size and compare with previous results as well.[78,82] Moreover, we show the evolution of the pressure in the liquid as a function of the size of the solid cluster during its formation for systems I and X, and as can be seen, there are two crosses corresponding to the extrema in ΔF. In this work, we focus on describing the connection between the stable nuclei in the NVT ensemble and nucleation. Thus, we are describing the nuclei at the minimum of ΔF. However, the maximum could certainly be used as a description of nucleation as well.

The phase coexistence of phases with curved interfaces is usually represented with a phase coexistence diagram where the chemical potential is plotted against the packing fraction $\phi = \rho\pi/6$. In Fig. 7, we show this kind of description. We show systems I and X. As can be seen, the region given by ϕ at which one can have a certain type of geometry is limited and this geometry can be either stable or metastable there. In the case of system I, only the homogeneous liquid and the planar interface can be obtained as global minimum. In the case of system X, one can have all configurations as global minimum depending on ϕ.

Once we have tested the theory in the ten cases considered in our previous work, obtaining good agreement, we use the theory to extensively describe the nucleation of hard spheres in a finite system as well as the phase coexistence of the solid and liquid in the NVT ensemble, which includes spherical, cylindrical, and planar coexistence. Note that these are two sides of the same coin since

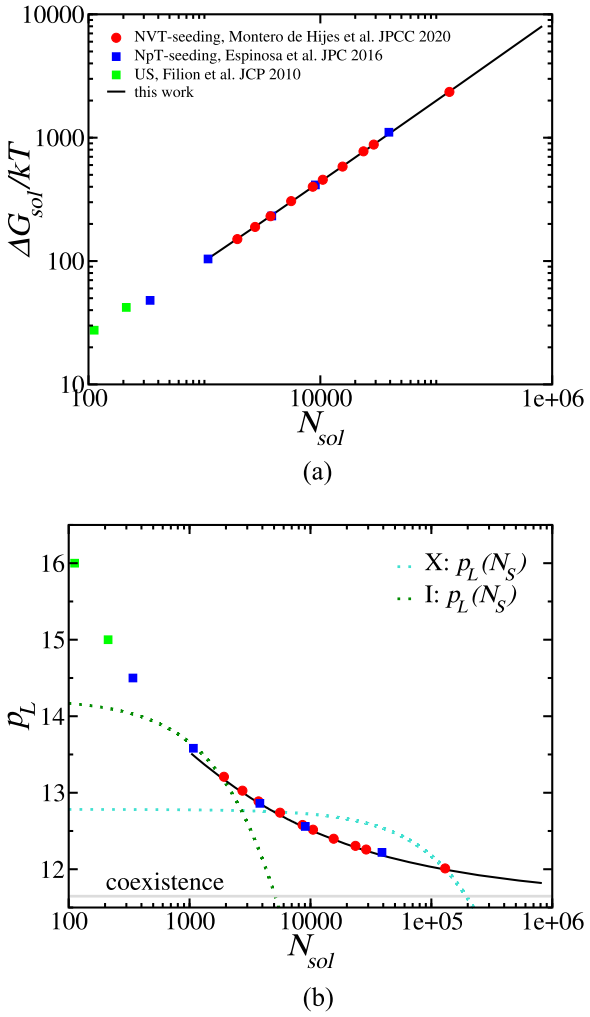

FIG. 6. (a) ΔG_{sol} as a function of the critical nucleus size N_{sol}. (b) Liquid pressure at which the solid cluster is a critical nucleus as a function of N_{sol}. The same legend from (a) applies in (b) although in the latter two additional dashed curves are shown. These correspond to the pressure of the liquid along the formation of a solid cluster of size N_S in systems I (green dashed line) and X (cyan dashed line). As can be seen, there are two crossings between these lines and the equilibrium one corresponding to $N_S = N_{sol}$. The crossing at smaller N_{sol} corresponds to the maximum in ΔF and the one at the larger N_{sol} corresponds to the minimum. In addition, the pressure of critical nucleus approaches (planar) coexistence for an infinite system as expected.

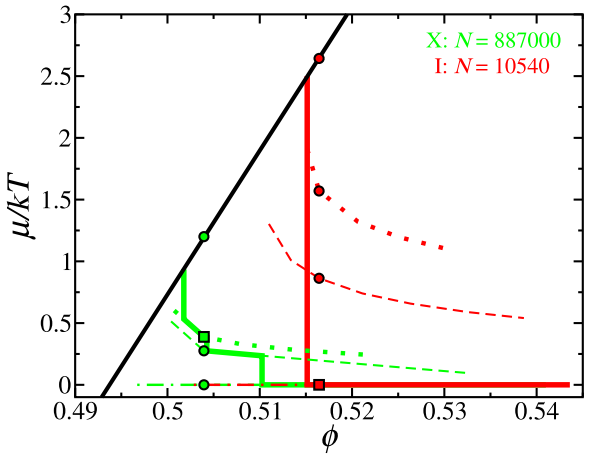

FIG. 7. Chemical potential μ against packing fraction $\phi = (\pi/6)(N/V)$. The black curve shows $\mu(\phi)$ for the bulk liquid. Then, the coexistence of phases is represented for two different system sizes. Two different sizes as given by N are studied. The volume V is changed covering different packing fractions ϕ. One size studied is the one of system I (in red) and the other is the one of system X (in green). Dotted lines represent the region of the coexistence of spherical nuclei with liquid. Dashed lines represent the region of coexistence of cylindrical nuclei with liquid. The dashed-dotted line represents the region of coexistence of planar solid–liquid interfaces. The thick solid red and solid green curves connect the points where a certain geometry is the most stable one, i.e., it is the global minimum. Any other point is metastable for the given system. Also shown are the values corresponding to the minima of systems I and X, respectively, in circles when they are local minima and in squares when they are the global minima.

the coexistence of a spherical solid nucleus with liquid can also be regarded as the study of a critical nucleus in ensembles where the chemical potential of the external phase is constant after changing the size of the nucleus.

For instance, it is interesting to analyze how the size of the stable spherical solid clusters is affected by the conditions of the system or under which conditions the sphere is more stable than the cylinder or the planar geometry. Key variables to describe the system are N, V, $\rho = N/V$, or even N_{sol}. We shall now fix one of these variables and analyze how the properties of the system at equilibrium can be affected by changing one of the other three variables, for instance, what happens when keeping N fixed while one changes V. In Fig. 8(a), the profiles of seven systems with the same N and different V are shown. As can be seen, the larger the volume, the smaller the stable-critical nucleus. In addition, these smaller nuclei are less stable with respect to the homogeneous liquid. Thus, at fixed N, increasing the global density ρ increases the number of particles of the phase whose density is larger (crystal) and vice versa. Hence, $(\partial N_{sol}/\partial V)_N < 0$. In this exercise, V ranged between $19\,850\sigma^3$ and $20\,450\sigma^3$, whereas $N = 20\,000$. Our next analysis is about what happens in the equilibrium solid cluster when keeping V constant while changing N. In this case, again the global density leads the way N_{sol} changes so that $(\partial N_{sol}/\partial N)_V > 0$. Results are shown in Fig. 8(b). In this case, N ranged between 19 750 and 20 300, whereas $V^* = 20\,150$. Thus, increasing the density of the system by changing either N or V and keeping the other variable constant increase the size of the spherical solid cluster. Now, we investigate the effect of keeping ρ constant by changing both V and N accordingly. As can be seen in Fig. 8(c), increasing the system size (both N and V to keep ρ constant) dramatically affects the size of the stable spherical solid cluster N_{sol} at constant ρ. The number of particles in the system ranged between 60 000 and 1 200 000 while $\rho = 0.97$. Increasing the size of the system increases the size of the stable solid cluster at constant ρ. Thus, the density alone does not determine the value of N_{sol}.

To continue with the analysis, we investigate the possibility of having several systems (differing in N, V, and ρ) having the same size of the stable solid cluster N_{sol}. We do so by changing both V and N, ensuring that we obtain the same value N_{sol}. In Fig. 9(a), we show

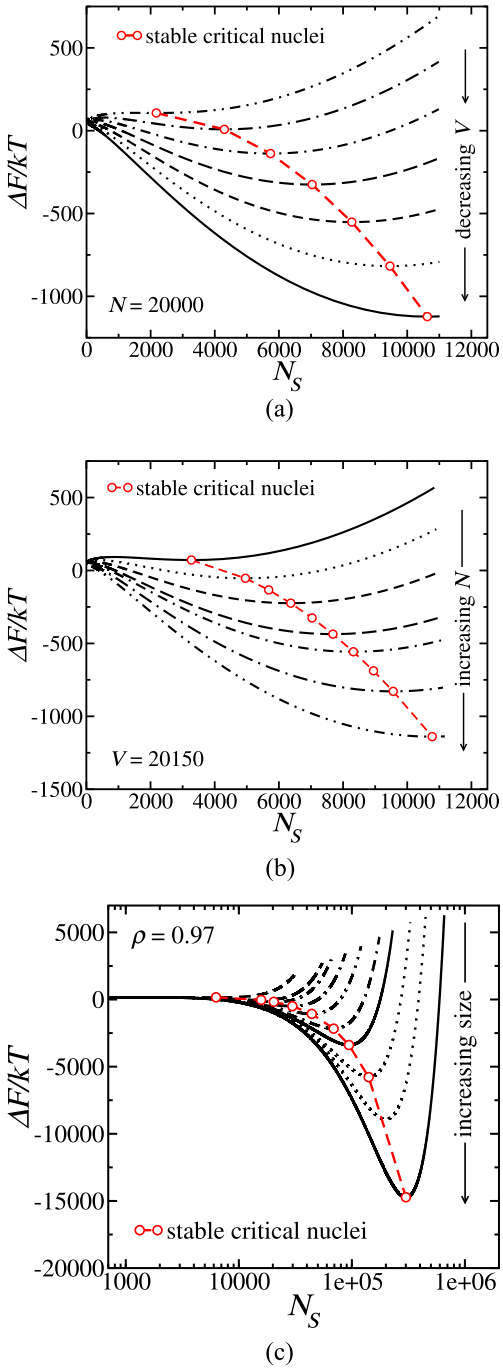

FIG. 8. ΔF as a function of the number of crystalline particles N_S for different systems sharing the same (a) total number of particles N, (b) system volume V, and (c) global density ρ.

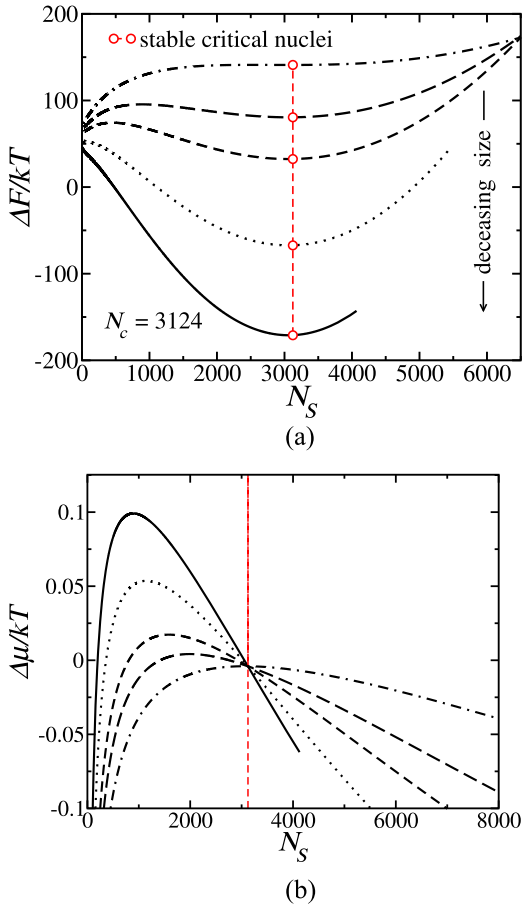

FIG. 9. (a) ΔF and (b) $\Delta\mu$ as a function of the number of crystalline particles N_S for different systems where stable-critical nuclei are all the same.

the free energy curve ΔF, and in (b), we show the chemical potential difference for systems with different conditions that lead to the same N_{sol}. As can be seen, the free energy curve can be very different for a single stable-critical nucleus. In fact, we have seen that the values of p_L at the minimum of ΔF are the same regardless of the size of the system. However, at some point, we are in a inflection point for ΔF when the system is sufficiently large. It is interesting to note that in the case when both extrema merge into a single point, then the curves like those in Fig. 5 would become tangential to the dependence of liquid pressure at which a solid cluster is a critical nucleus. In Fig. 9(b), this effect can be seen from the fact that $\Delta\mu$ is tangential to zero at N_{sol}. Note that ΔG_{sol} is the same in all the cases as given by $A(R^s_{sol})\gamma^s/3$. However, it is clear that it is not possible to have any stable solid cluster beyond a certain size of the system so that one cannot make the system arbitrarily large. In fact, we always found in our previous study that the ratio N_{sol}/N for all the cases where the spherical solid cluster was stable for a certain time was between 0.05 and 0.20. We never succeeded in getting this ratio below 0.05. This is well explained in Fig. 9(a) as when one increases N, while keeping N_{sol} constant, the local minimum in ΔF is lost at some point. On the other hand, when the system is too small, we also expect that no nucleus is stable at some point.

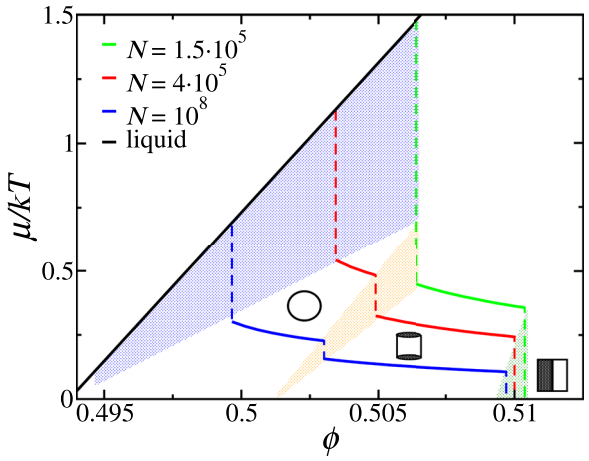

FIG. 10. Chemical potential μ of the most stable geometry at certain finite conditions against the resulting packing fraction for three different systems characterized by $N = 1.5 \cdot 10^5$ (green), $N = 4 \cdot 10^5$ (red), and $N = 10^8$ (blue). In black, μ of the homogeneous liquid which only depends on ϕ. The region where a certain geometry dominates depends on the system size. Dashed areas represent the transition region between equilibrium configurations (homogeneous liquid ↔ sphere in liquid, sphere in liquid ↔ cylinder in liquid, and cylinder in liquid ↔ planar interface). Note that we assigned $\mu = 0$ for the liquid and solid phases at the coexistence pressure of the bulk phases (as when separated by a planar interface).

To conclude, following the work of Binder and co-workers,[27] we compute the chemical potential μ of the most stable configuration of a certain system (homogeneous liquid or sphere/cylinder/slab in contact with liquid) for a certain global packing fraction $\phi = \rho\pi/6$ for different finite systems characterized by N. These results are shown in Fig. 10. Let us focus on the system composed by 10^8 hard spheres. For $\phi < 0.4997$, the homogeneous liquid is the most stable configuration, i.e., it is the global minimum. Then, at $0.4997 < \phi \leq 0.5030$, we find the sphere surrounded by liquid as the most stable configuration; at $0.5030 < \phi \leq 0.5097$, the cylinder wins; and finally, above 0.5097, the planar slab takes over. We can see that for systems where $N < 1.5 \cdot 10^5$, the sphere is never the equilibrium state and can exist only as a metastable state. Another observation is that with increasing system size, the chemical potential approaches the (planar) coexistence one as the curvature effects become small.

V. CONCLUSIONS

In this work, we propose a thermodynamic treatment to describe the change in the Helmholtz free energy F as a function of the size of the solid cluster N_S. In particular, we use the Gibbsian formalism extended by Tolman, Kondo, Mullins, and Rowlinson and Widom. We include simulation inputs though. These are the equations of state and the change of both the interfacial free energy and the distance between the equimolar and tension surfaces with curvature. In particular, we apply it to a system of hard spheres at constant N, V, and T. We use the thermodynamics of curved interfaces at equilibrium to describe the whole energy profile so that only extrema are actually quantitatively relevant. The rest of the curve is interesting but only qualitatively. Despite being far from the coexistence point (for planar interface), we observe different local minima corresponding to different configurations of the system which can be a homogeneous liquid or a spherical, cylindrical, or planar solid cluster in contact with liquid. We observe that the transition between these configurations are via activated processes. In addition, we observe that, depending on the thermodynamic conditions of the system, a certain configuration is the equilibrium state and, in some cases, the free energy barrier between the metastable liquid and the equilibrium state is so large that intermediate states with smaller barriers are visited even though they are actually less stable than the metastable liquid in what reminds us to an Ostwald-like process. By setting the conditions to the same as in previous simulation results, we obtain the stable solid cluster size, pressures, and densities, finding excellent agreement with the simulations for spherical, cylindrical, and planar geometries. In the simulation results, it was shown that the stable nucleus in the NVT ensemble is critical in the NpT ensemble. Once we validate our approach, we use it to extensively describe the stabilization of nucleation solid clusters of hard spheres in a finite system. First of all, we obtain the dependence of the Gibbs free energy barrier with the size of the stable-critical nucleus. Then, we evaluate the effect that a certain variable has over nucleation in a finite system. We estimate the Helmholtz free energy curves for systems sharing a certain parameter: N, V, ρ, or N_{sol}. We show that if one fixes either N or V and vary the other, then if ρ increases, the phase with larger density, in this case the crystal, grows in number (i.e., N_{sol} increases) and vice versa. Moreover, we observe that ρ alone does not explain the size of the stable nucleus as also N or V are needed. At constant ρ, systems of different size present very different sizes of the stable nucleus. Another finding is that one can have the same stable-critical nucleus in different finite systems, but the stability is not the same. Actually, at some point, the maximum and the minimum merge forming an inflection point. Thus, one can stabilize a certain nucleus only in a certain range of system parameters. Finally, we compute the chemical potential of the most stable phase at certain finite conditions, and we show that we need at least 150 000 hard spheres in order to achieve a spherical solid cluster as global minimum. There, a paradoxical critical state can actually last indefinitely in the absence of external perturbation. We observe that the larger the system, the closer the chemical potential is to the planar coexistence value as curvature gets more and more negligible.

We hope that more studies aimed at investigating the equilibrium of curved interfaces (specially spherical ones) in the NVT ensemble follow on, taking into account that by doing that one is studying the critical cluster found in nucleation studies.

SUPPLEMENTARY MATERIAL

See the supplementary material for finding a Fortran code that is provided. This code allows one to compute the approximated Helmholtz free energy profile of a liquid of hard spheres in which a solid cluster emerges (at constant N, V, and T). This allows one to determine the Helmholtz free energy of the solid cluster at equilibrium (and from there, the Gibbs free energy barrier for nucleation at constant pressure and temperature).

ACKNOWLEDGMENTS

We thank Professor E. Sanz for useful comments and discussions on this work. P.M.d.H. acknowledges financial support from the FPI (Grant No. BES-2017-080074). The authors acknowledge Project No. PID2019–105898GB-C21 of the Ministerio de Educacion y Cultura.

AUTHOR DECLARATIONS

Conflict of Interest

The authors have no conflicts to disclose.

DATA AVAILABILITY

The data that support the findings of this study are available from the corresponding author upon reasonable request.

APPENDIX A: CLASSICAL NUCLEATION THEORY

The Classical Nucleation Theory (CNT) aims at describing homogeneous nucleation.[75,93] The key magnitude in nucleation is the nucleation rate J which represents the number of critical nuclei that appear per unit of time and volume. CNT was developed by Volmer–Weber and Becker–Doring[71,72,75,94] and defines J as

$$J_{CNT} = K_0 \exp\left(-\frac{\Delta G_c}{kT}\right), \tag{A1}$$

where K_0 is a kinetic term well described in classical books[75] and where $\exp(-\Delta G_c/kT)$ is a thermodynamic term that is usually described with the Gibbsian formalism. In particular, ΔG_c is the free energy barrier to nucleation. Even though CNT includes both kinetic and thermodynamic terms and certainly J is a kinetic magnitude, in many occasions, CNT refers to the description of the free energy barrier ΔG_c. In a previous work, we showed that the stable nucleus in the NVT ensemble was critical in the NpT ensemble.[35] Thus, stable nuclei can be used to study nucleation so that there must be a connection between the formalism used in this work and CNT.

The Gibbs free energy of a homogeneous liquid formed by N particles, at pressure p_L whose chemical potential is μ_L, is given by

$$G_{homogeneous} = N\mu_L. \tag{A2}$$

When a solid nucleus appears, the system becomes inhomogeneous. Since we want to connect the formalism of curved interfaces and CNT, we use the Helmholtz free energy F of the stable nucleus to describe the Gibbs free energy of a critical nucleus as

$$G_{inhomogeneous} = F + p_L V, \tag{A3}$$

where F is given by Eq. (4). Note that the pressure that we have used in the thermodynamic conversion between F and G is that of the liquid. This has been discussed by Yang,[95] and we have recently shown (see the Supplementary Material of Ref. 56) that the average pressure in the simulation equals that of the liquid when the mechanical equilibrium condition ($\nabla \cdot \mathbf{p} = 0$) is fulfilled. Thus, we have

$$G_{inhomogeneous} = N\mu_L - p^{\mu}_{sol} V_{sol} - p_L V_L + \gamma A_{sol} + p_L V. \tag{A4}$$

Now, we can compute the Gibbs free energy barrier as the difference between the inhomogeneous and the homogeneous systems, $\Delta G_c = G_{inhomogeneous} - G_{homogeneous}$. This leads to

$$\Delta G_c = \gamma A_{sol} - V_{sol}(p^{\mu}_{sol} - p_L) = \gamma A_{sol} - V_{sol}\Delta p^{\mu}. \tag{A5}$$

Here, ΔG_c is well defined just like F in Eq. (4), and in this case, there is also arbitrariness in the location of the dividing surface which affects γ. Thus, one can apply Eq. (A5) for any dividing surface as long as the corresponding γ is used. For instance, one can use R^e_{sol} as long as the value of γ that one applies is γ^e or R^s_{sol} if γ^s is used. In fact, by taking the notational derivative of ΔG_c (i.e., an arbitrary change in R_{sol} without any physical change in the system so that $[d\Delta G_c/dR_{sol}] = 0$), one recovers Eq. (6). By using the surface of tension R^s_{sol}, one obtains the Young–Laplace equation [Eq. (7)], and by substituting in Eq. (A5), one obtains

$$\Delta G_c = \frac{1}{3}\gamma^s A^s = \frac{1}{2} V^s \Delta p^{\mu}, \tag{A6}$$

where $A^s = 4\pi(R^s_{sol})^2$ and $V^s = (4/3)\pi(R^s_{sol})^3$.

Equation (A6) is one of the main equations of CNT, and we have found it using the thermodynamic formalism of curved interfaces in equilibrium in the NVT ensemble. As a matter of fact, the critical nucleus and surrounding liquid are in thermodynamic equilibrium of the unstable kind in the NpT ensemble.

It can be shown easily that $\Delta F(N_{sol})$ (relevant to study equilibrium) is related to ΔG_c (relevant to study nucleation) by the following expression:[39]

$$\Delta F_{sol} = \Delta G_c + N\left(\mu_L - \mu^0_L\right) + V\left(p^0_L - p_L\right). \tag{A7}$$

What is the right dividing surface to consider in CNT? Let us assume that γ is known for a given dividing surface in a certain critical nucleus. Let us assume also that for the thermodynamic conditions (p, T) of the system, γ does not change with the size of the solid embryo that at some point becomes a critical nucleus. We can approximate the free energy profile as

$$\Delta G = 4\pi R^2 \gamma - \frac{4}{3}\pi R^3 \Delta p^{\mu}, \tag{A8}$$

where $\Delta p^{\mu} = p^{\mu}_{sol} - p_L$. By setting the derivative with respect to R equal to zero, we find the condition of maximum (where $\Delta G = \Delta G^*$)

$$R^* = \frac{2\gamma}{\Delta p^{\mu}}. \tag{A9}$$

If γ, which we assumed to be constant, is γ^s, then

$$R^{*s} = \frac{2\gamma^s}{\Delta p^{\mu}} = R^s \tag{A10}$$

as given by the Young–Laplace equation, allowing us identify that $R^{*s} = R^s$. By substituting in Eq. (A5) the values R^s and γ^s, we recover ΔG_c since both γ and R refer to the same dividing surface. Hence, $R^{*s} = R^s$ and $\Delta G_c = \Delta G^{*s}$. However, if we assume that $\gamma = \gamma^e$, then

$$R^{*e} = \frac{2\gamma^e}{\Delta p^{\mu}} \neq R^e \neq R^s \tag{A11}$$

as can be seen by comparing with the generalized Young–Laplace equation. Now, if in Eq. (A5) we use γ^e and R^e, we obtain the right value of ΔG_c, but if we use γ^e and R^{*e}, we obtain a value of ΔG in the maximum ΔG^{*e} that is different to ΔG_c since γ and R do not refer to the same dividing surface in this case since $R^e \neq R^{*e}$. Therefore, the dividing surface corresponding to the maximum that gives a consistent value of ΔG_c is R^s. Thus, the dividing surface to consider in nucleation when using CNT is the surface of tension R^s_{sol} and the interfacial free energy is γ^s. A sketch of this is shown in Fig. 11. There, the approximated free energy profile for constant $\gamma = \gamma^s$ (in blue) and for $\gamma = \gamma^e$ (in red) is shown.

If we substitute R^s given as $R^s = (2\gamma^s)/\Delta p^\mu$ and the corresponding $\gamma = \gamma^s$ in Eq. (A8), we obtain another important equation in CNT,

$$\Delta G_c = \frac{16\pi(\gamma^s)^3}{3(\Delta p^\mu)^2}. \tag{A12}$$

If one assumes that the solid is incompressible (so that its density does not change with pressure), then it can be shown that $\Delta p^\mu \simeq \rho_{sol}\Delta\mu^{CNT}$, where $\Delta\mu^{CNT}$ is the difference in chemical potential between a bulk liquid and a bulk solid having both the same pressure p_L. One can then replace Δp^μ by its approximate expression in Eq. (A12) or in Eq. (A5) obtaining

$$\Delta G_c = \frac{16\pi(\gamma^s)^3}{3(\rho_{sol}\Delta\mu^{CNT})^2}, \tag{A13}$$

$$\Delta G_c = \gamma A_{sol} - V_{sol}\rho_{sol}\Delta\mu^{CNT} = \gamma A_{sol} - N_{sol}\Delta\mu^{CNT}. \tag{A14}$$

In fact, one sees Eq. (A13) more often than Eq. (A12) in CNT formalism although the latter is, in general, better since it does not use the incompressibility approximation. In fact, Eq. (A12) was the one proposed by Gibbs to describe the free energy barrier[55,96] and should be used whenever is possible.

How to feed the formalism of CNT with results obtained from simulations ? This is the approach of seeding where one determines

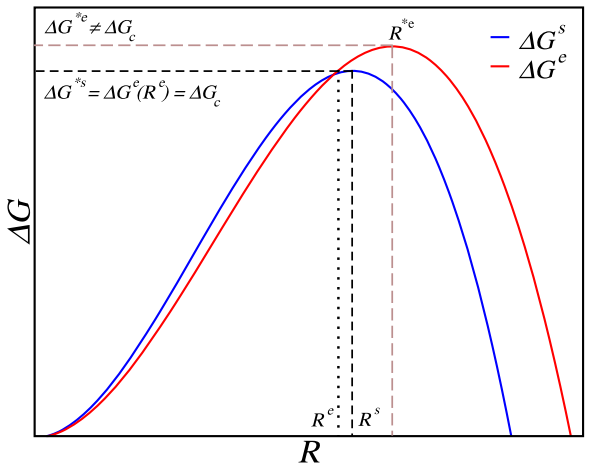

FIG. 11. Schematic representation of approximated Gibbs free energy profiles where γ is assumed to be constant.

that a certain cluster is indeed critical. By using the simple equation (A6), one could determine the value of the free energy barrier ΔG_c. Δp^μ can be obtained from the EOS of the fluid and solid and the value of p_{coex}. Therefore, the problem is to evaluate the volume of the critical cluster evaluated at the radius of its surface of tension, namely, V^s. This can be done once we know the number of particles of the solid cluster, and then V^s is given by N_{sol}/ρ_{sol}. Typically, one uses an order parameter that labels the molecules as solid or liquid[97] and determines the size of the critical cluster N_{sol}. The problem arises from the fact that different order parameters provide different values of N_{sol} for the same physical cluster. One should select one that estimates correctly the volume at the surface of tension of the cluster. When this is done, CNT should reproduce the results obtained from more rigorous techniques such as umbrella sampling,[76–78] transition path sampling,[98] metadynamics,[99] or forward flux sampling[78,100] for free energy barriers and nucleation rates J. In short, CNT with adequate feeding (i.e., a correct estimate of the radius of tension) can provide a good description of nucleation rates as obtained from more rigorous techniques. However, this requires a certain tuning of the choice of the order parameter in order to estimate correctly the radius at the surface of tension of the critical cluster.

Along similar lines, Reguera and Wedekind[101] suggested that a good order parameter should be the one that satisfies the so called first nucleation theorem stating that[75,102–104]

$$d\,(kT\ln(J))/d\Delta\mu^{CNT} = N_c + c = \rho_{sol}V^s + c. \tag{A15}$$

Note that the left-hand side term does not depend on any arbitrary choice of surfaces. Both the nucleation rates and $\Delta\mu^{CNT}$ are experimental and well determined properties. However, the term on the right-hand side depends on the order parameter. Once again, to satisfy this theorem, one should use an order parameter that provides a value of $N_{sol} = N_c$ able to estimate R^s_{sol} correctly. The value of c is usually small and accounts for the change of the kinetic pre-factor K_0 and of γ with $\Delta\mu^{CNT}$.

In our opinion, some of the arguments often used against CNT are not fully correct. It is sometimes stated that it assumes that the solid is incompressible [this criticism is not valid when one uses Eq. (A12) since this equation already proposed by Gibbs does not require to assume that], that it is wrong as the properties of the actual solid are not those of a bulk solid (this criticism is not correct as the properties of the actual solid never enter in CNT but rather those of a bulk solid with the same chemical potential of the fluid phase), that γ^s is constant (this is not correct as one could and should incorporate the change of γ^s with the radius of curvature), or that it does not describe the complete free energy profile for the formation of a solid cluster at constant p and T (this is true, but the purpose of CNT is not to describe this profile but just the value of the free energy barrier at the maximum, namely, ΔG_c, which is the property needed to estimate J). Although for certain cases CNT may fail due to a complex mechanism for freezing,[105,106] in most of the cases, it should provide good estimates of the nucleation rate, provided that one is able to determine the location of the radius of tension for the problem of interest. This is the key limitation of CNT as only rigorous free energy calculations can determine this radius. However, educated order parameters can provide a reasonable guess transforming CNT into a useful tool. Gibbs is still guiding us.[107]

APPENDIX B: STATISTICAL MECHANICS VS THERMODYNAMICS

The phase space with all possible configurations in the NVT ensemble can be partitioned using an order parameter like the number of solid particles of the largest solid cluster N_S. That allows one to obtain a free energy profile as

$$F(N_s) = -kT \ln(Q(N_S)), \tag{B1}$$

where $Q(N_S)$ is the canonical partition function. Therefore, the value of $F(N_S)$ can be obtained rigorously by evaluating the expression

$$F(N_S) = -kT \ln \int \exp\left(-\beta U\left(R^{3N}\right)\right) \times \delta\left(N_S^*\left(R^{3N}\right) - N_S\right) dR^{3N} + C, \tag{B2}$$

where $N_S^*(R^{3N})$ is the number of particles in the solid cluster for an instantaneous configuration as given by the coordinates of all particles of the system R^{3N} and C is a constant. This could be done, for instance, by using umbrella sampling (US)[76,77] or metadynamics.[99] However, the implementation is far from trivial. In fact, US calculations were implemented in the past but only to estimate the free energy for clusters having around 200 hard sphere particles.[76,77] In the case of water, this number increases up to 400 molecules[108] for the mW model.[109] This difficulty arises because the free energy barrier increases with the critical nucleus size. The size of the solid clusters that we were able to stabilize in the NVT ensemble for HS in our previous study ranges between 2000 particles (the smallest one) and around 800 000.[35] Therefore, the evaluation of $F(N_S)$ for these large values of N_S is extremely expensive from a computational point of view although further work along this line is needed in the future.

Of course, the rigorous free energy of the system should be obtained by including in the configurational integral all possible configurations (i.e., $F = -kT \ln[Q(N_s = 0) + Q(N_s = 1) + \cdots + Q(N_s = N)]$. Let us assume that the free energy profile (as a function of N_s) has one or several local minima. One of them will be the global minimum. Then, if the global minimum is quite deep in the free energy landscape, one can approximate the rigorous value of F by considering only those configurations thermally accessible (say, within 10–15 kT) from the global minimum. In this case, the rigorous free energy of the system can be approximated considering only those configurations close to the global minimum. However, it is also useful to define the free energy of the system around a local minimum when there are large free energy barriers separating these local minima. The system can stay in these local minima for long times, and one can define the free energy for this metastable configuration, provided that the time to pass the free energy barrier is much higher than the time to relax and equilibrate around the local minimum. This is equivalent to why one can define thermodynamic properties of supercooled water (at moderate supercooling), provided that the relaxation time is lower than the nucleation time even though the configurational integral is dominated by the solid configurations. Technically, one determines this free energy by considering only configurations around the local minimum. Therefore a thermodynamic description of these local minima is possible. A schematic representation of these local minima can be found in Fig. 12. The dashed areas correspond to configurations accessible from thermal fluctuations of up to 10–15 kT. There, the thermodynamic description is possible since the system stays for a long time. However, let us focus on the magenta circle. From a statistical mechanics point of view, that represents a configuration with low probability to be obtained via fluctuations from the equilibrium system. From a thermodynamical point of view, this configuration is not in equilibrium since the chemical potentials of the solid and the liquid are different (see Fig. 4).

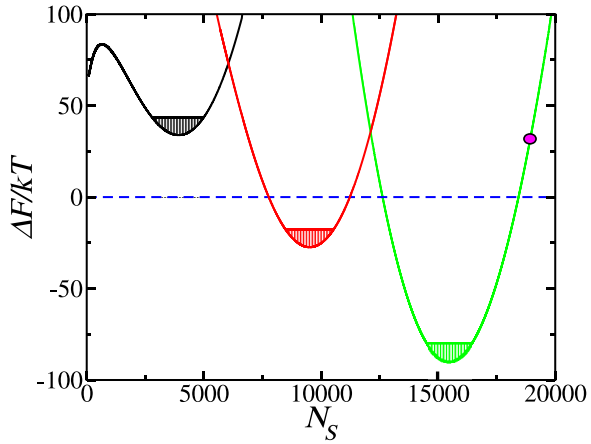

FIG. 12. Schematic representation of approximated Helmholtz free energy profiles against the size of solid spherical (black), cylindrical (red), and planar (green) nucleus in contact with liquid. The dashed colored regions around the local minima represent fluctuations up to 10–15 kT. There, a thermodynamic description is possible. The magenta circle represents a configuration far from any minimum so that a thermodynamic description is only approximated at that point. This configuration is seen from a statistical mechanics point of view as a configuration with little probability that can be reached via fluctuations at equilibrium and from a thermodynamics point of view as being that of a system at non-equilibrium as the chemical potential of both phases is different at this configuration (the difference in chemical potential being given by $d\Delta F/dN_S$).

REFERENCES

[1] E. M. Blokhuis and J. Kuipers, "Thermodynamic expressions for the Tolman length," J. Chem. Phys. **124**, 074701 (2006).
[2] B. J. Block, S. K. Das, M. Oettel, P. Virnau, and K. Binder, "Curvature dependence of surface free energy of liquid drops and bubbles: A simulation study," J. Chem. Phys. **133**, 154702 (2010).
[3] J. G. Sampayo, A. Malijevský, E. A. Müller, E. de Miguel, and G. Jackson, "Evidence for the role of fluctuations in the thermodynamics of nanoscale drops and the implications in computations of the surface tension," J. Chem. Phys. **132**, 141101 (2010).
[4] A. Malijevský and G. Jackson, "A perspective on the interfacial properties of nanoscopic liquid drops," J. Phys.: Condens. Matter **24**, 464121 (2012).
[5] A. Tröster, M. Oettel, B. Block, P. Virnau, and K. Binder, "Numerical approaches to determine the interface tension of curved interfaces from free energy calculations," J. Chem. Phys. **136**, 064709 (2012).
[6] H. M. Lu and Q. Jiang, "Size-dependent surface tension and Tolman's length of droplets," Langmuir **21**, 779–781 (2005).
[7] S. M. Thompson, K. E. Gubbins, J. P. R. B. Walton, R. A. R. Chantry, and J. S. Rowlinson, "A molecular dynamics study of liquid drops," J. Chem. Phys. **81**, 530 (1984).
[8] G. V. Lau, I. J. Ford, P. A. Hunt, E. A. Müller, and G. Jackson, "Surface thermodynamics of planar, cylindrical, and spherical vapour-liquid interfaces of water," J. Chem. Phys. **142**, 114701 (2015).

[9]J. Vrabec, G. K. Kedia, G. Fuchs, and H. Hasse, "Comprehensive study of the vapour-liquid coexistence of the truncated and shifted Lennard-Jones fluid including planar and spherical interface properties," Mol. Phys. **104**, 1509 (2006).
[10]Ø. Wilhelmsen, D. Bedeaux, and D. Reguera, "Tolman length and rigidity constants of the Lennard-Jones fluid," J. Chem. Phys. **142**, 064706 (2015).
[11]M. N. Joswiak, R. Do, M. F. Doherty, and B. Peters, "Energetic and entropic components of the Tolman length for mW and TIP4P/2005 water nanodroplets," J. Chem. Phys. **145**, 204703 (2016).
[12]J. W. P. Schmelzer, A. S. Abyzov, and V. G. Baidakov, "Entropy and the Tolman parameter in nucleation theory," Entropy **21**, 670 (2019).
[13]D. Richard and T. Speck, "Crystallization of hard spheres revisited. II. Thermodynamic modeling, nucleation work, and the surface of tension," J. Chem. Phys. **148**, 224102 (2018).
[14]K. G. S. H. Gunawardana and X. Song, "Theoretical prediction of crystallization kinetics of a supercooled Lennard-Jones fluid," J. Chem. Phys. **148**, 204506 (2018).
[15]A. O. Tipeev, "Comment on 'theoretical prediction of crystallization kinetics of a supercooled Lennard-Jones fluid [J. Chem. Phys. 148, 204506 (2018)],'" J. Chem. Phys. **151**, 017101 (2019).
[16]K. G. S. H. Gunawardana and X. Song, "Response to 'comment on theoretical prediction of crystallization kinetics of a supercooled Lennard-Jones fluid [J. Chem. Phys. 151, 017101 (2019)],'" J. Chem. Phys. **151**, 017102 (2019).
[17]P. Bryk, R. Roth, K. R. Mecke, and S. Dietrich, "Hard-sphere fluids in contact with curved substrates," Phys. Rev. E **68**, 031602 (2003).
[18]N. Di Pasquale and R. L. Davidchack, "Shuttleworth equation: A molecular simulations perspective," J. Chem. Phys. **153**, 154705 (2020).
[19]S. Kondo, "Thermodynamical fundamental equation for spherical interface," J. Chem. Phys. **25**, 662 (1956).
[20]J. S. Rowlinson and B. Widom, *Molecular Theory of Capillarity* (Courier Corporation, 2013).
[21]A. J. M. Yang, "The thermodynamical stability of the heterogeneous system with a spherical interface," J. Chem. Phys. **82**, 2082–2085 (1985).
[22]A. I. Rusanov, "The thermodynamics of processes of new-phase formation," Russ. Chem. Rev. **33**, 385–399 (1964).
[23]D. J. Lee, M. M. Telo da Gama, and K. E. Gubbins, "A microscopic theory for spherical interfaces: Liquid drops in the canonical ensemble," J. Chem. Phys. **85**, 490–499 (1986).
[24]D. W. Oxtoby and R. Evans, "Nonclassical nucleation theory for the gas-liquid transition," J. Chem. Phys. **89**, 7521 (1988).
[25]M. Schrader, P. Virnau, and K. Binder, "Simulation of vapor-liquid coexistence in finite volumes: A method to compute the surface free energy of droplets," Phys. Rev. E **79**, 061104 (2009).
[26]M. Schrader, P. Virnau, D. Winter, T. Zykova-Timan, and K. Binder, "Methods to extract interfacial free energies of flat and curved interfaces from computer simulations," Eur. Phys. J.: Spec. Top. **177**, 103–127 (2009).
[27]K. Binder, B. J. Block, P. Virnau, and A. Tröster, "Beyond the Van der Waals loop: What can be learned from simulating Lennard-Jones fluids inside the region of phase coexistence," Am. J. Phys. **80**, 1099–1109 (2012).
[28]A. Statt, P. Virnau, and K. Binder, "Finite-size effects on liquid-solid phase coexistence and the estimation of crystal nucleation barriers," Phys. Rev. Lett. **114**, 026101 (2015).
[29]A. Tröster and K. Binder, "Positive Tolman length in a lattice gas with three-body interactions," Phys. Rev. Lett. **107**, 265701 (2011).
[30]P. Koß, A. Statt, P. Virnau, and K. Binder, "The phase coexistence method to obtain surface free energies and nucleation barriers: A brief review," Mol. Phys. **116**, 2977–2986 (2018).
[31]P. Koß, A. Statt, P. Virnau, and K. Binder, "Free-energy barriers for crystal nucleation from fluid phases," Phys. Rev. E **96**, 042609 (2017).
[32]P. Virnau, F. Schmitz, and K. Binder, "The ensemble switch method and related approaches to obtain interfacial free energies between coexisting phases from simulations: A brief review," Mol. Simul. **42**, 549–562 (2016).
[33]A. Tröster, F. Schmitz, P. Virnau, and K. Binder, "Equilibrium between a droplet and surrounding vapor: A discussion of finite size effects," J. Phys. Chem. B **122**, 3407–3417 (2017).
[34]P. Rosales-Pelaez, I. Sanchez-Burgos, C. Valeriani, C. Vega, and E. Sanz, "Seeding approach to nucleation in the NVT ensemble: The case of bubble cavitation in overstretched Lennard-Jones fluids." Phys. Rev. E **101**, 022611 (2020).
[35]P. Montero de Hijes, J. R. Espinosa, V. Bianco, E. Sanz, and C. Vega, "Interfacial free energy and Tolman length of curved solid-liquid interfaces from equilibrium studies," J. Phys. Chem. C **124**, 8795 (2020).
[36]I. Sanchez-Burgos, P. M. de Hijes, P. Rosales-Pelaez, C. Vega, and E. Sanz, "Equivalence between condensation and boiling in a Lennard-Jones fluid," Phys. Rev. E **102**, 062609 (2020).
[37]D. Reguera, R. K. Bowles, Y. Djikaev, and H. Reiss, "Phase transitions in systems small enough to be clusters," J. Chem. Phys. **118**, 340 (2003).
[38]J. F. Lutsko, "How crystals form: A theory of nucleation pathways," Sci. Adv. **5**, eaav7399 (2019).
[39]V. G. Baidakov, "Phase equilibria in a microheterogeneous liquid–gas system: Gibbs capillary model," Chem. Phys. **525**, 110407 (2019).
[40]A. K. Shchekin, K. Koga, and N. A. Volkov, "The effect of a finite number of monomers available for aggregation at nucleation and micellization in a fixed volume," J. Chem. Phys. **151**, 244903 (2019).
[41]L. A. Zepeda-Ruiz, B. Sadigh, A. A. Chernov, T. Haxhimali, A. Samanta, T. Oppelstrup, S. Hamel, L. X. Benedict, and J. L. Belof, "Extraction of effective solid-liquid interfacial free energies for full 3D solid crystallites from equilibrium MD simulations," J. Chem. Phys. **147**, 194704 (2017).
[42]L. G. MacDowell, P. Virnau, M. Müller, and K. Binder, "The evaporation/condensation transition of liquid droplets," J. Chem. Phys. **120**, 5293 (2004).
[43]L. G. MacDowell, V. K. Shen, and J. R. Errington, "Nucleation and cavitation of spherical, cylindrical, and slablike droplets and bubbles in small systems," J. Chem. Phys. **125**, 034705 (2006).
[44]J. Jover, A. J. Haslam, A. Galindo, G. Jackson, and E. A. Müller, "Pseudo hard-sphere potential for use in continuous molecular-dynamics simulation of spherical and chain molecules," J. Chem. Phys. **137**, 144505 (2012).
[45]P. Rosales-Pelaez, P. M. de Hijes, E. Sanz, and C. Valeriani, "Avalanche mediated devitrification in a glass of pseudo hard-spheres," J. Stat. Mech.: Theory Exp. **2016**, 094005.
[46]J. R. Espinosa, E. Sanz, C. Valeriani, and C. Vega, "On fluid-solid direct coexistence simulations: The pseudo-hard sphere model," J. Chem. Phys. **139**, 144502 (2013).
[47]J. R. Espinosa, C. Vega, and E. Sanz, "The mold integration method for the calculation of the crystal-fluid interfacial free energy from simulations," J. Chem. Phys. **141**, 134709 (2014).
[48]P. Montero de Hijes, J. R. Espinosa, E. Sanz, and C. Vega, "Interfacial free energy of a liquid-solid interface: Its change with curvature," J. Chem. Phys. **151**, 144501 (2019).
[49]B. Hess, C. Kutzner, D. van der Spoel, and E. Lindahl, "GROMACS 4: Algorithms for highly efficient, load-balanced, and scalable molecular simulation," J. Chem. Theory Comput. **4**, 435–447 (2008).
[50]S. Plimpton, J. Comput. Phys. **117**, 1 (1995).
[51]S. Ono and S. Kondo, "Molecular theory of surface tension in liquids," in *Structure of Liquids/Struktur der Flüssigkeiten* (Springer, 1960), pp. 134–280.
[52]W. W. Mullins, "Thermodynamic equilibrium of a crystalline sphere in a fluid," J. Chem. Phys. **81**, 1436–1442 (1984).
[53]C. Perego, O. Valsson, and M. Parrinello, "Chemical potential calculations in non-homogeneous liquids," J. Chem. Phys. **149**, 072305 (2018).
[54]J. S. Rowlinson, "Thermodynamics of inhomogeneous systems," Pure Appl. Chem. **65**, 873 (1993).
[55]J. Gibbs, *The Collected Works. Volume 1. Thermodynamics* (Yale University Press, 1948).
[56]P. Montero de Hijes, K. Shi, E. G. Noya, E. E. Santiso, K. E. Gubbins, E. Sanz, and C. Vega, "The Young–Laplace equation for a solid–liquid interface," J. Chem. Phys. **153**, 191102 (2020).
[57]J. W. Cahn, "Surface stress and the chemical equilibrium of small crystals—I. The case of the isotropic surface," Acta Metall. **28**, 1333–1338 (1980).
[58]R. C. Cammarata, "Generalized thermodynamics of surfaces with applications to small solid systems," Solid State Phys. **61**, 1 (2009).
[59]P. R. ten Wolde and D. Frenkel, "Computer simulation study of gas-liquid nucleation in a Lennard-Jones system," J. Chem. Phys. **109**, 9901 (1998).

[60]I. M. Klotz and T. F. Young, *Introduction to Chemical Thermodynamics* (W. A. Benjamin, 1964).
[61]R. C. Tolman, "The effect of droplet size on surface tension," J. Chem. Phys. **17**, 333–337 (1949).
[62]A. Cacciuto, S. Auer, and D. Frenkel, "Breakdown of classical nucleation theory near isostructural phase transitions," Phys. Rev. Lett. **93**, 166105 (2004).
[63]A. Cacciuto and D. Frenkel, "Stresses inside critical nuclei," J. Phys. Chem. B **109**, 6587–6594 (2005).
[64]M. J. P. Nijmeijer, C. Bruin, A. B. Van Woerkom, A. F. Bakker, and J. M. J. Van Leeuwen, "Molecular dynamics of the surface tension of a drop," J. Chem. Phys. **96**, 565–576 (1992).
[65]X.-S. Wang and R.-Z. Zhu, "A method to calculate the surface tension of a cylindrical droplet," Eur. J. Phys. **31**, 79 (2009).
[66]B. B. Laird, R. L. Davidchack, Y. Yang, and M. Asta, "Determination of the solid-liquid interfacial free energy along a coexistence line by Gibbs-Cahn integration," J. Chem. Phys. **131**, 114110 (2009).
[67]T. Dreher, N. Pineau, E. Bourasseau, P. Malfreyt, L. Soulard, and C. A. Lemarchand, "Anisotropic surface stresses of a solid/fluid interface: Molecular dynamics calculations for the copper/methane interface," J. Chem. Phys. **151**, 244703 (2019).
[68]E. M. Blokhuis and D. Bedeaux, "Pressure tensor of a spherical interface," J. Chem. Phys. **97**, 3576 (1992).
[69]G. A. Chapela, G. Saville, S. M. Thompson, and J. S. Rowlinson, "Computer simulation of a gas–liquid surface. Part 1," J. Chem. Soc., Faraday Trans. 2 **73**, 1133 (1977).
[70]J. G. Kirkwood and F. P. Buff, "The statistical mechanical theory of surface tension," J. Chem. Phys. **17**, 338 (1949).
[71]M. Volmer and A. Weber, "Keimbildung in ubersattigten gebilden," Z. Phys. Chem. **119U**, 277 (1926).
[72]R. Becker and W. Döring, "Kinetische behandlung der keimbildung in ubersattigten dampfen," Ann. Phys. **416**, 719–752 (1935).
[73]D. Turnbull, "Formation of crystal nuclei in liquid metals," J. Appl. Phys. **21**, 1022–1028 (1950).
[74]D. Turnbull, "Kinetics of solidification of supercooled liquid mercury droplets," J. Chem. Phys. **20**, 411 (1952).
[75]K. F. Kelton and A. L. Greer, *Nucleation in Condensed Matter* (Pergamon, Elsevier, Oxford, 2010).
[76]S. Auer and D. Frenkel, "Prediction of absolute crystal-nucleation rate in hard-sphere colloids," Nature **409**, 1020 (2001).
[77]S. Auer and D. Frenkel, "Quantitative prediction of crystal-nucleation rates for spherical colloids: A computational approach," Annu. Rev. Phys. Chem. **55**, 333 (2004).
[78]L. Filion, M. Hermes, R. Ni, and M. Dijkstra, "Crystal nucleation of hard spheres using molecular dynamics, umbrella sampling, and forward flux sampling: A comparison of simulation techniques," J. Chem. Phys. **133**, 244115 (2010).
[79]X.-M. Bai and M. Li, "Calculation of solid-liquid interfacial free energy: A classical nucleation theory based approach," J. Chem. Phys. **124**, 124707 (2006).
[80]B. C. Knott, V. Molinero, M. F. Doherty, and B. Peters, "Homogeneous nucleation of methane hydrates: Unrealistic under realistic conditions," J. Am. Chem. Soc. **134**, 19544–19547 (2012).
[81]E. Sanz, C. Vega, J. R. Espinosa, R. Caballero-Bernal, J. L. F. Abascal, and C. Valeriani, "Homogeneous ice nucleation at moderate supercooling from molecular simulation," J. Am. Chem. Soc. **135**, 15008–15017 (2013).
[82]J. R. Espinosa, C. Vega, C. Valeriani, and E. Sanz, "Seeding approach to crystal nucleation," J. Chem. Phys. **144**, 034501 (2016).
[83]J. R. Espinosa, A. Zaragoza, P. Rosales-Pelaez, C. Navarro, C. Valeriani, C. Vega, and E. Sanz, "Interfacial free energy as the key to the pressure-induced deceleration o f ice nucleation," Phys. Rev. Lett. **117**, 135702 (2016).
[84]Y. Sun, H. Song, F. Zhang, L. Yang, Z. Ye, M. I. Mendelev, C. Z. Wang, and K. M. Ho, "Overcoming the time limitation in molecular dynamics simulation of crystal nucleation: A persistent-embryo approach," Phys. Rev. Lett. **120**, 085703 (2018).
[85]A. O. Tipeev, E. D. Zanotto, and J. P. Rino, "Diffusivity, interfacial free energy, and crystal nucleation in a supercooled Lennard-Jones liquid," J. Phys. Chem. C **122**, 28884–28894 (2018).
[86]S. Burian, M. Isaiev, K. Termentzidis, V. Sysoev, and L. Bulavin, "Size dependence of the surface tension of a free surface of an isotropic fluid," Phys. Rev. E **95**, 062801 (2017).
[87]C. Vega and E. G. Noya, "Revisiting the Frenkel-Ladd method to compute the free energy of solids: The Einstein molecule approach," J. Chem. Phys. **127**, 154113 (2007).
[88]D. Frenkel and B. Smit, *Understanding Molecular Simulation* (Academic Press, London, 1996).
[89]R. J. Speedy, "Pressure and entropy of hard-sphere crystals," J. Phys.: Condens. Matter **10**, 4387 (1998).
[90]R. L. Davidchack, J. R. Morris, and B. B. Laird, "The anisotropic hard-sphere crystal-melt interfacial free energy from fluctuations," J. Chem. Phys. **125**, 094710 (2006).
[91]Ø. Wilhelmsen, D. Bedeaux, S. Kjelstrup, and D. Reguera, "Communication: Superstabilization of fluids in nanocontainers," J. Chem. Phys. **141**, 071103 (2014).
[92]T. Philippe, "Nucleation and superstabilization in small systems," Phys. Rev. E **96**, 032802 (2017).
[93]D. Kashchiev, *Nucleation: Basic Theory with Applications* (Butterworth-Heinemann, Oxford, 2000).
[94]S. Jungblut and C. Dellago, "Pathways to self-organization: Crystallization via nucleation and growth," Eur. Phys. J. E **39**, 77 (2016).
[95]A. J. M. Yang, "Free energy for the heterogeneous systems with spherical interfaces," J. Chem. Phys. **79**, 6289–6293 (1983).
[96]D. Kashchiev, "Nucleation work, surface tension, and Gibbs–Tolman length for nucleus of any size," J. Chem. Phys. **153**, 124509 (2020).
[97]W. Lechner and C. Dellago, "Accurate determination of crystal structures based on averaged local bond order parameters," J. Chem. Phys. **129**, 114707 (2008).
[98]P. G. Bolhuis, D. Chandler, C. Dellago, and P. L. Geissler, "Transition path sampling: Throwing ropes over rough mountain passes, in the dark," Annu. Rev. Phys. Chem. **53**, 291 (2002).
[99]A. Barducci, G. Bussi, and M. Parrinello, "Well-tempered metadynamics: A smoothly converging and tunable free-energy method," Phys. Rev. Lett. **100**, 020603 (2008).
[100]R. J. Allen, D. Frenkel, and P. R. ten Wolde, "Simulating rare events in equilibrium or nonequilibrium stochastic systems," J. Chem. Phys. **124**, 024102 (2006).
[101]D. Reguera and J. Wedekind, "What is the best definition of a liquid cluster at the molecular scale?," J. Chem. Phys. **127**, 154516 (2007).
[102]D. Kashchiev, "On the relation between nucleation work, nucleus size, and nucleation rate," J. Chem. Phys. **76**, 5098 (1982).
[103]D. W. Oxtoby and D. Kashchiev, "A general relation between the nucleation work and the size of the nucleus in multicomponent nucleation," J. Chem. Phys. **100**, 7665 (1994).
[104]J. W. P. Schmelzer, "Application of the nucleation theorem to crystallization of liquids: Some general theoretical results," Entropy **21**, 1147 (2019).
[105]H. Jiang, P. G. Debenedetti, and A. Z. Panagiotopoulos, "Nucleation in aqueous NaCl solutions shifts from 1-step to 2-step mechanism on crossing the spinodal," J. Chem. Phys. **150**, 124502 (2019).
[106]G. C. Sosso, J. Chen, S. J. Cox, M. Fitzner, P. Pedevilla, A. Zen, and A. Michaelides, "Crystal nucleation in liquids: Open questions and future challenges in molecular dynamics simulations," Chem. Rev. **116**, 7078 (2016).
[107]R. de Miguel and J. M. Rubí, "Gibbs thermodynamics and surface properties at the nanoscale," J. Chem. Phys. **155**, 221101 (2021).
[108]J. Russo, F. Romano, and H. Tanaka, "New metastable form of ice and its role in the homogeneous crystallization of water," Nat. Mater. **13**, 733–739 (2014).
[109]V. Molinero and E. B. Moore, "Water modeled as an intermediate element between carbon and silicon," J. Phys. Chem. B **113**, 4008–4016 (2009).